THE ROLE OF DEFECTS IN THE QUANTUM SIZE EFFECT

DISSERTATION

Presented to the Graduate Council of the
North Texas State University in Partial
Fulfillment of the Requirements

For the Degree of

DOCTOR OF PHILOSOPHY

By

Farris D. Malone, B. S., M. S.
Denton, Texas
December, 1974

WDD

Malone, Farris D., The Role of Defects in the Quantum Size Effect. Doctor of Philosophy (Physics), December, 1974, 52 pp., 1 table, 9 illustrations, 56 references.

This investigation is a theoretical study of the influence of defects of finite volume on the electrical conductivity in the quantum size effect regime. Correction terms to existing equations are derived, and a physical explanation of the results is given.

Many macroscopic properties of films exhibit an oscillatory dependence on thickness when the thickness is comparable to the de Broglie wavelength of an electron at the Fermi surface. This behavior is called the quantum size effect. In very thin films, scattering from surfaces, phonons, and crystal defects plays an increasingly important role. In this investigation the influence of scattering centers (defects) in semimetal films on the electrical conductivity is explored by extending existing work to include scattering centers of finite range. The purpose of this study is to determine the overall change in the conductivity and the alteration of the amplitude of the oscillations.

The Boltzmann transport equation is the starting point for the calculation. An equation for the vector mean free path is derived, and a solution is obtained by the iterative process. The relaxation approximation need not be made since the vector mean free path is determined.

The sample is a thin slab that is infinite in two dimensions. The assumption is made that the electron wave function is zero at the walls of the sample. It is further assumed that there is a known number of randomly located defects within the slab. The noninteracting electrons are considered free except in the vicinity of the scattering centers. The defects are characterized by a potential that is constant within a small cube and zero outside of it. This approach allows the potential matrix elements to be evaluated by expanding in a power series.

The electrical conductivity is calculated for three defect sizes, and a comparison is made to δ-function (infinitely small) scattering centers. An overall decrease in the conductivity is found in each case, and the absolute magnitude of the oscillations is decreased. The percentage of oscillation, however, is increased. The general conductivity decrease is attributed to the increase in the scattering range. The change in the amplitude of the oscillations is explained by analyzing the transition probabilities to available energy states at critical film thicknesses. The oscillations are found to be a result of transitions from states with large energies in the plane of the film to states with small energies in the plane of the film. The number of electrons occupying the various states is determined at critical film thicknesses, and a comparison with the conductivity equation shows excellent agreement.

TABLE OF CONTENTS

LIST OF TABLES

LIST OF ILLUSTRATIONS

CHAPTER I

INTRODUCTION

In very thin solid films, macroscopic properties, such as conductivity, Hall coefficient, and optical parameters, exhibit an oscillatory dependence on the film thickness. The oscillations occur when the film thickness is comparable to the de Broglie wavelength of an electron at the Fermi surface. This behavior is called the quantum size effect (QSE) and is based on the quantization of the carrier momentum that is normal to the film plane.

The possibility of size oscillations in some thermodynamic characteristics was predicted by Lifshitz and Kaganov.[1,2] Oscillations in the resistivity resulting from quantization due to magnetic fields led them to conjecture that if the sample is thin enough, the size of the film can quantize the momentum and cause oscillations. Tavger and Demikhovskii consider the problem in depth and evaluate the conditions under which QSE can be observed.[3] Sandomirskii comments in more detail on the sample thickness in metals and semiconductors necessary for the detection of QSE.[4] These evaluations lead to the increased importance of having detailed knowledge of the semimetal and semiconductor band structures and Fermi surfaces. Kao provides useful information in his investigation of the Fermi surface of bismuth.[5] Esaki and Stiles

further study this semimetal by investigating its electronic band structure.[6]

Ogrin, Lutskii, and Elinson were the first to experimentally observe the oscillations.[7] Their data on bismuth films includes work with magnetic fields as well as variations in sample thickness. The initial experimental QSE observation was followed by many accounts of oscillatory dependence. To date these effects have been reported in antimony,[8] aluminum,[9] indium antimonide,[10] and copper sulfide.[11] Thin inversion layers in silicon[12,13] and alloyed mercury-cadmium-tellurium compounds[14] have been studied. Ugaz and Soonpaa discuss the conductivity in thin crystals of a bismuth-tellurium-sulfur compound.[15] The bulk of experimental work, however, has been concerned with bismuth, specifically the trigonal surface.

The oscillatory effects have been investigated under a variety of conditions. Duggal, Rup, and Tripathi[16] observe oscillations in thin bismuth films similar to those previously observed by Ogrin, Lutskii, and Elinson. Oscillations in longitudinal magnetoresistance in single crystalline bismuth films are reported by Garcia, Kao, and Strongin,[17] by Bogod and Eremenko,[18] and by Lal and Duggal.[19] Vatamanyuk, Kulyupin, and Sarbei employ high electric fields to explore QSE.[20] Lutskii and Kulik find oscillations in the optical absorption of bismuth films.[21] Fesenko uses differential magnetoresistance to investigate bismuth films, and observes QSE oscillations.[22] He also discusses high-frequency oscillations which

he attributes to the hole part of the Fermi surface.[23] An x-ray investigation of the bismuth surface is made by Konczak, Kochowski, and Ziolowski on samples in which oscillations have been observed.[24] Komnik and Bukhshtab note QSE in polycrystalline bismuth films.[25] They find that the conductivity increases as the film thickness decreases, a distinct feature not normally observed. Asahi, Humoto, and Kawazu compare experimental results with the high-temperature anisotropic theory and generally find agreement.[26] The temperature dependence of the resistivity is also considered by Ogrin et al. by comparing theoretical and experimental results for thin bismuth films.[27] Using an anisotropic model, Gol'dfarb and Tavger explain the experimentally observed features of the Hall constant on thickness.[28] Size effects have been studied in contact potential[29] as well as in tunneling experiments.[30] All of these experimental results give acceptable values for the effective mass and Fermi energy in bismuth.

Sandomirskii provides solid mathematical groundwork for the oscillatory effects at low temperature.[31] Kulik calculates the conductivity as a function of sample thickness, using quantum field theory methods,[32] and arrives at substantially the same results as Sandomirskii. The theory for QSE at high temperature for an anisotropic sample is given by Nedorezov,[33] while Erukhimov and Tavger work out the theory for longitudinal galvanomagnetic phenomena in thin films.[34] Krishnan and Meyer derive an expression for the conductivity in the case

of a magnetic field perpendicular to the plane of the film.[35] Shik calculates the conductivity when electrons are scattered by a screened coulomb potential.[36] Bezak derives the formula for the Fermi energy for thin films[37] and generalizes Fuchs' theory by deriving a quantum mechanical expression for the electrical current.[38]

Quantum size effects are reviewed briefly by Tavger,[39] then more extensively by Tavger and Demikhovskii.[40] A review of experimental investigations into the oscillatory effects is given by Lutskii.[41] Possible practical applications of QSE are discussed by Elinson et al.[42]

Most of the experimental work is concerned with semimetals and heavily doped semiconductors, since the effect can be observed with reasonably thick ($\cong 10^{-5}$ cm) films. The effect is most prominent at very low temperature and is damped out as the temperature is increased. There have been, however, several experimental observations of oscillatory effects in the conductivity at room temperature.[43-45]

At very low temperature the resistivity increases rapidly as the thickness decreases. Simple theory indicates that at a sample thickness of one-half the Fermi wavelength, the resistivity goes to infinity in the ideal case. The increase is due to band overlap removal. The semimetal undergoes a transition to a semiconductor. Many experimental observations indicate that the transition has probably been observed[21,44-47]; however, some data show a broad maximum in the resistivity

even for very thin films where the transition to a semiconductor should have occurred.[48] Garcia, Kao, and Strongin point out that the requirement for band overlap removal can be lifted if the assumption is made that the surface of the film can be penetrated by conduction electrons, thus allowing a lower subband of energy levels to exist.[17]

Many of the relevant features of QSE are shown in Fig. 1. The low-frequency oscillations (period $\cong$ 400 Å) are a result of variations in electron state density, while the high-frequency oscillations (period $\cong$ 50 Å) are probably due to the hole part of the Fermi surface. Bulk samples of bismuth show a metallic resistivity temperature dependence, but bismuth films show a resistivity increase with a decrease in temperature. A plot of the resistivity in bismuth exhibits a minimum which decreases with temperature and with structural perfection of the film.

Very thin films present both experimental and theoretical problems. Scattering from lattice vibrations, surfaces, and defects may play an increasingly important role as the film becomes thinner.[49-51] Compared to the results obtained by using a δ-function scattering potential,[31] scattering from defects of finite size should produce two changes in the electrical conductivity at low temperature. There should be a general decrease in the conductivity, and the amplitude of the oscillations should be altered. The purpose of this

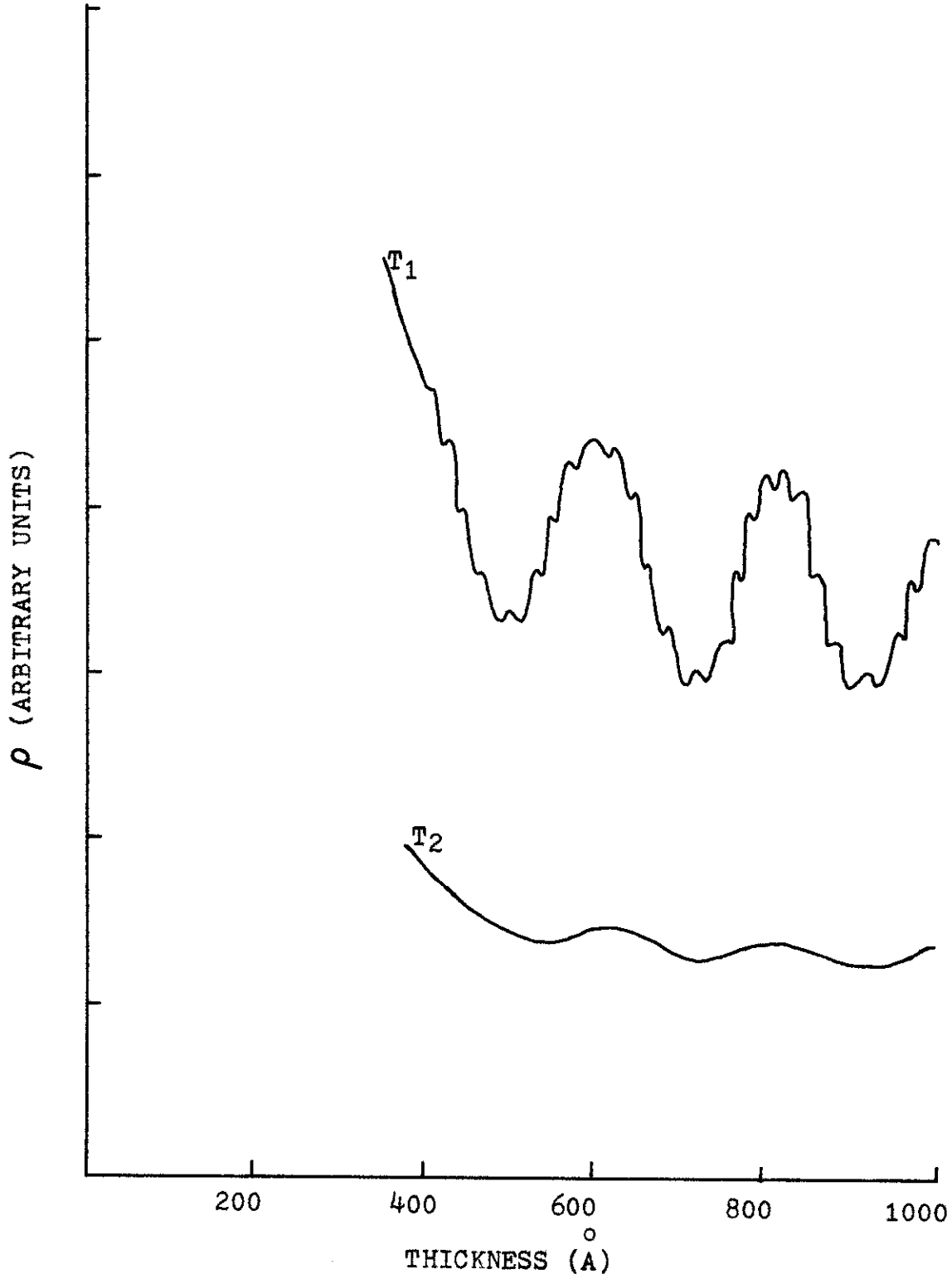

Fig. 1. Idealized resistance trace showing the quantum size effects. The upper curve is for a temperature denoted by T_1, and the lower curve is for a temperature T_2 with $T_2 > T_1$.

investigation is to demonstrate that these effects occur for a potential of finite range. The relaxation approximation will not be made. The vector mean free path will be calculated, and correction terms to existing theories will be generated.

CHAPTER II

DERIVATION OF THE CONDUCTIVITY EQUATION

In this investigation the electrical conductivity of a solid slab is calculated. It is assumed that there are no magnetic fields or temperature gradients within the solid. Scattering from lattice vibrations (phonons) is neglected, but scattering from defects of finite volume is taken into account. The electron distribution function $f_{\vec{k}}$, which gives the number of electrons in the state $\vec{k}$, under steady state conditions is given by

$$\frac{\partial f_{\vec{k}}}{\partial t} = 0. \tag{1}$$

The changes in $f_{\vec{k}}$ resulting from the electric field $\vec{E}$ must therefore be offset by the changes caused by scattering from defects. This condition can be written as

$$\left.\frac{\partial f_{\vec{k}}}{\partial t}\right|_{sc} + \left.\frac{\partial f_{\vec{k}}}{\partial t}\right|_{field} = 0. \tag{2}$$

The change with time of the distribution function as a result of the electric field is

$$\left.\frac{\partial f_{\vec{k}}}{\partial t}\right|_{field} = -\frac{\partial f_{\vec{k}}}{\partial \vec{K}} \cdot \frac{\partial \vec{K}}{\partial t} = -\frac{e\vec{E}}{\hbar} \cdot \frac{\partial f_{\vec{k}}}{\partial \vec{K}}. \tag{3}$$

The rate of change of $f_{\vec{k}}$ as a result of impurity scattering

is the average net number of electrons entering the state $\vec{k}$ from all other states $\vec{k}'$. Then the term $\partial f_{\vec{k}}/(\partial t)|_{sc}$ can be expressed as

$$\left.\frac{\partial f_{\vec{k}}}{\partial t}\right|_{sc} = \sum_{\vec{k}'}\left[f_{\vec{k}'}\,Q(\vec{k},\vec{k}')\left(1-f_{\vec{k}}\right) - f_{\vec{k}}\,Q(\vec{k}',\vec{k})\left(1-f_{\vec{k}'}\right)\right] \tag{4}$$

where $Q(\vec{k},\vec{k}')$ is the transition probability per unit time of scattering from the state $\vec{k}$ to the state $\vec{k}'$. Using the fact $Q(\vec{k},\vec{k}') = Q(\vec{k}',\vec{k})$ simplifies Eq. (4) to

$$\left.\frac{\partial f_{\vec{k}}}{\partial t}\right|_{sc} = \sum_{\vec{k}'} Q(\vec{k},\vec{k}')\left(f_{\vec{k}'}-f_{\vec{k}}\right). \tag{5}$$

The assumption is made that the steady state distribution does not depart far from the equilibrium, i.e.

$$f_{\vec{k}} = f^{o}_{\vec{k}} + f'_{\vec{k}} \tag{6}$$

where $f^{o}_{\vec{k}}$ is the Fermi-Dirac distribution function. For elastic scattering, Schiff's equation[52] for the function $Q(\vec{k},\vec{k}')$ can be written

$$Q(\vec{k},\vec{k}') = \frac{2\pi}{\hbar}\left|\langle\vec{k}|V|\vec{k}'\rangle\right|^{2}\delta\left(E_{\vec{k}}-E_{\vec{k}'}\right) \tag{7}$$

where $E_{\vec{k}}$ is the energy of the state having momentum $\hbar\vec{k}$. The term $|\langle\vec{k}|V|\vec{k}'\rangle|^{2}$ is the square of the potential matrix elements. Inserting Eqs. (6) and (7) into Eq. (5) results in

$$\left.\frac{\partial f_{\vec{k}}}{\partial t}\right|_{sc} = \left.\frac{\partial f'_{\vec{k}}}{\partial t}\right|_{sc}$$

$$= \sum_{\vec{k}'} Q(\vec{k},\vec{k}')\left(f'_{\vec{k}'}-f'_{\vec{k}}\right). \tag{8}$$

After the application of Eqs. (3) and (5), Eq. (2) becomes

$$\sum_{\vec{K}'} Q(\vec{K},\vec{K}')\left(f'_{\vec{K}} - f'_{\vec{K}'}\right) = \frac{e\vec{E}}{\hbar} \cdot \frac{\partial f_{\vec{K}}}{\partial \vec{K}}$$

$$= \frac{e\vec{E}}{\hbar} \cdot \frac{\partial f_{\vec{K}}}{\partial E_{\vec{K}}} \frac{\partial E_{\vec{K}}}{\partial \vec{K}} . \tag{9}$$

Equation (9) further simplifies to

$$\sum_{\vec{K}'} Q(\vec{K},\vec{K}')\left(f'_{\vec{K}} - f'_{\vec{K}'}\right) = e\vec{E} \cdot \vec{v}_{\vec{K}} \frac{\partial f_{\vec{K}}}{\partial E_{\vec{K}}} . \tag{10}$$

The right side of Eq. (10) is altered by inserting Eq. (6). Under these conditions Eq. (10) can be written

$$\sum_{\vec{K}'} Q(\vec{K},\vec{K}')\left(f'_{\vec{K}} - f'_{\vec{K}'}\right) = e\vec{E} \cdot \vec{v}_{\vec{K}} \frac{\partial f^{0}_{\vec{K}}}{\partial E_{\vec{K}}} \tag{11}$$

where the term involving the product of $f'_{\vec{K}}$ and $\vec{E}$ has been neglected so that only terms linear in $\vec{E}$ remain. At low temperature the right side of Eq. (11) is different from zero only if $E_{\vec{K}}$ is $E_{\vec{f}}$ (the Fermi energy). A function $\vec{\Lambda}_{\vec{K}}$ is defined as

$$f'_{\vec{K}} = -e\vec{E} \cdot \vec{\Lambda}_{\vec{K}} \frac{\partial f^{0}_{\vec{K}}}{\partial E_{\vec{K}}} \tag{12}$$

where $\vec{\Lambda}_{\vec{K}}$ is independent of $\vec{E}$. Using Eq. (12) in Eq. (11) results in

$$\sum_{\vec{K}'} Q(\vec{K},\vec{K}')\left(\vec{\Lambda}_{\vec{K}} - \vec{\Lambda}_{\vec{K}'}\right) = \vec{v}_{\vec{K}} . \tag{13}$$

Solving Eq. (13) for $\vec{\Lambda}_{\vec{K}}$ gives

$$\vec{\Lambda}_{\vec{K}} = \frac{\vec{v}_{\vec{K}}}{U_{\vec{K}}} + \frac{1}{U_{\vec{K}}} \sum_{\vec{K}'} Q(\vec{K},\vec{K}')\vec{\Lambda}_{\vec{K}'} \tag{14}$$

where $U_{\vec{K}}$ has been written for $\sum_{\vec{K}'} Q(\vec{k},\vec{k}')$.

The total current density J can be expressed as

$$\vec{J} = \Omega^{-1}\sum_{\vec{k}} e\,\vec{v}_{\vec{k}}\, f_{\vec{k}}$$

$$= \Omega^{-1}\sum_{\vec{k}} e\,\vec{v}_{\vec{k}}\, f'_{\vec{k}} = -\frac{e^2}{\Omega}\sum_{\vec{k}} \vec{v}_{\vec{k}}\,\vec{\Lambda}_{\vec{k}}\cdot\vec{E}\,\frac{\partial f^{o}_{\vec{k}}}{\partial E_{\vec{k}}}. \qquad (15)$$

The conductivity $\overleftrightarrow{\sigma}$ can be determined from

$$\vec{J} = \overleftrightarrow{\sigma}\cdot\vec{E}. \qquad (16)$$

At low temperature the equation for the conductivity becomes

$$\overleftrightarrow{\sigma} = -\frac{e^2}{\Omega}\sum_{\vec{k}} \vec{\Lambda}_{\vec{k}}\,\vec{v}_{\vec{k}}\,\delta(E_{\vec{f}} - E_{\vec{k}}). \qquad (17)$$

Edwards derived a similar relation using the Greenwood-Peierls equation.[53] In doing so, he employed the Green's function of the Schrodinger equation which was evaluated by summing diagrams. The importance of that approach lies in the limited nature of the assumptions that must be made. In addition, diagrams are unique in accounting for all the interactions of a particular type. An excellent treatment of Edwards' work is given by Taylor.[54]

CHAPTER III

CHARACTERIZATION OF THE SAMPLE

The sample under investigation is a film having infinite dimensions in the x and y directions and a thickness L in the z direction ($0 \leq z \leq L$). Figure 2 shows a section of the sample. The potential walls bounding the sample are assumed to be infinite in height, and the effective mass m^* is assumed to be the same for all directions.

The single particle wave function is

$$\psi_{k_x,k_y,n} = \left(\frac{2}{LL_xL_y}\right)^{1/2} \sin(n\pi z/L)\, e^{i\vec{k}_\perp \cdot \vec{\rho}} \tag{18}$$

where $i\vec{k}_\perp \cdot \vec{\rho} = ik_x x + ik_y y$, L_x and L_y are the normalization lengths, $k_\perp$ is the continuous component of the momentum, and n is the quantum number associated with the component of the momentum that is perpendicular to the plane of the film.

The energy spectrum is given by

$$E_{k_\perp,n} = \hbar^2 k_\perp^2/(2m^*) + \alpha^2 n^2 \tag{19}$$

where $n = 1,2,3, \ldots$ and α^2 is $\pi^2\hbar^2/(2m^*L^2)$. Equation (19) shows that the energy spectrum is composed of bands, designated by n, within which there are continuous levels. The discrete part of the energy ($\alpha^2 n^2$) is associated with motion perpendicular to the plane of the film.

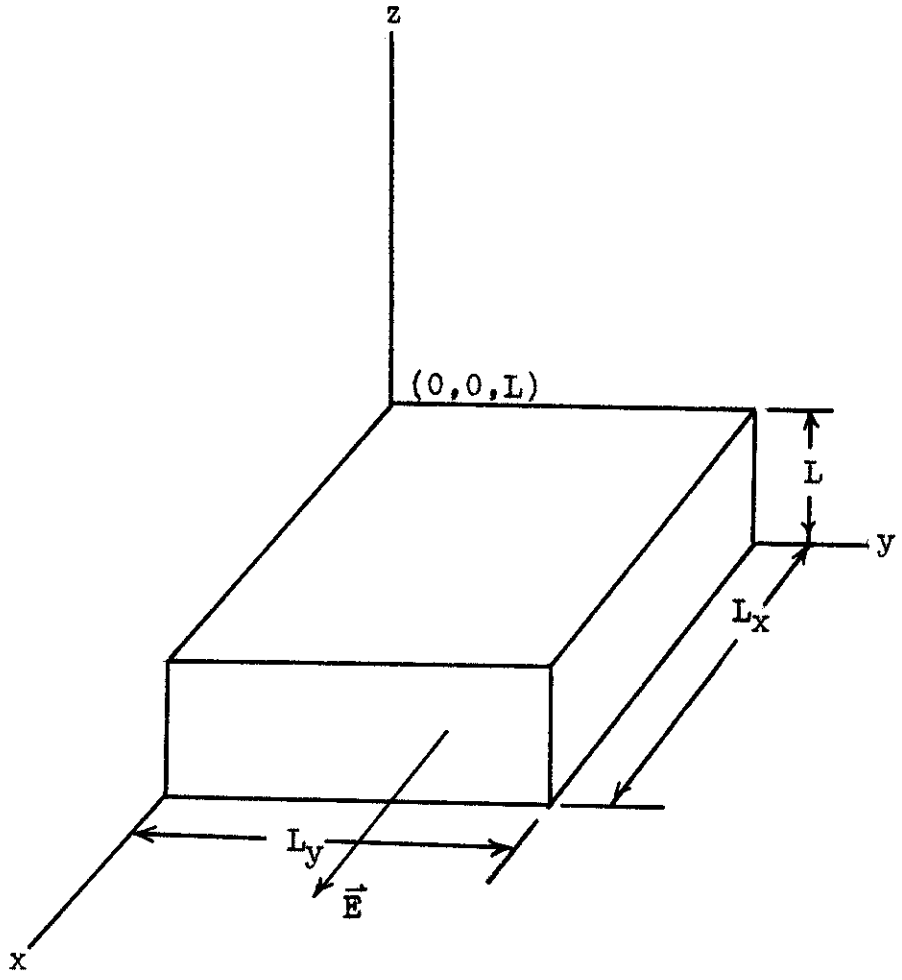

Fig. 2. A section of the thin slab for which the electrical conductivity is calculated. The direction of the electric field is shown by $\vec{E}$.

The total number of electrons N_e in the finite sample is

$$N_e = 2\sum_{\vec{K}} f(\vec{K}). \tag{20}$$

It is assumed that at low temperature all the momentum states are filled up to the Fermi energy but empty above it. Then the distribution function can be written as

$$f(\vec{K}) \cong \Theta(E_{\vec{f}} - E_{\vec{K}}) \tag{21}$$

where $E_{\vec{f}}$ is the Fermi energy. Equation (20) becomes

$$N_e \cong 2\sum_{\vec{K}} \Theta(E_{\vec{f}} - E_{\vec{K}}). \tag{22}$$

There are two continuous components of $\vec{k}$; therefore, $\sum_{\vec{k}}$ is replaced by $\left[L_x L_y/(2\pi)^2\right]\sum_n \int d\vec{k}_\perp$. The number of electrons in the film is

$$\begin{aligned} N_e &= \frac{2\Omega}{L(2\pi)^2}\sum_n \int d\vec{k}_\perp \Theta(E_{\vec{f}} - E_{\vec{K}}) \\ &= \frac{\Omega}{L(2\pi)^2}\sum_n \int_0^{2\pi} d\theta \int_0^{k_f^2 + \frac{2m^*}{\hbar^2}\alpha^2(n_f^2 - n^2)} dk_\perp^2 \\ &= \Omega m^* [N_f] (2\pi\hbar^2 L)^{-1}\left[E_f - \frac{\alpha^2}{6}(1+2[N_f])(1+[N_f])\right] \end{aligned} \tag{23}$$

with $[N_f]$ given as the largest integer less than or equal to $(E_f/\alpha^2)^{\frac{1}{2}}$ and Ω representing the volume of the film.

CHAPTER IV

SCATTERING POTENTIAL

The matrix elements for the scattering potential can now be calculated. The assumption is made that there are N randomly located scattering centers within the film. The scattering centers are characterized by a potential that is constant within a cube of volume $8a^3$. The potential (Fig. 3) is described by a step function for each coordinate, i.e.

$$V(\vec{r}) = -V_0 \sum_{i=1}^{N} \Theta(a-|x-x_i|)\Theta(a-|y-y_i|)\Theta(a-|z-z_i|) \tag{24}$$

with $\vec{r}_i = \vec{r}(x_i, y_i, z_i)$ as the scattering coordinate.

The matrix elements for the potential are given by

$$\langle \vec{k}|V|\vec{k}'\rangle = V_{\vec{k}\vec{k}'} = \int d\vec{r}\, d\vec{r}\,' \langle \vec{k}|\vec{r}\rangle\langle \vec{r}|V|\vec{r}\,'\rangle\langle \vec{r}\,'|\vec{k}'\rangle$$

$$= \int d\vec{r}\, d\vec{r}\,' \psi^{*}_{\vec{k}}(\vec{r})\, \psi_{\vec{k}'}(\vec{r}\,')\, V(\vec{r}\,')\, \delta(\vec{r}-\vec{r}\,')$$

$$= \int d\vec{r}\, \psi^{*}_{\vec{k}}(\vec{r})\, \psi_{\vec{k}'}(\vec{r})\, V(\vec{r}) \tag{25}$$

$$V_{\vec{k}\vec{k}'} = -V_0 |C|^2 \sum_{i=1}^{N} \int_{x_i-a}^{x_i+a} \exp(iq_x x)\, dx \int_{y_i-a}^{y_i+a} \exp(iq_y y)\, dy$$

$$\times \int_{z_i-a}^{z_i+a} \sin\left(\frac{n\pi z}{L}\right) \sin\left(\frac{n'\pi z}{L}\right) dz \tag{26}$$

where $q_x = k'_x - k_x$ and $q_y = k'_y - k_y$.

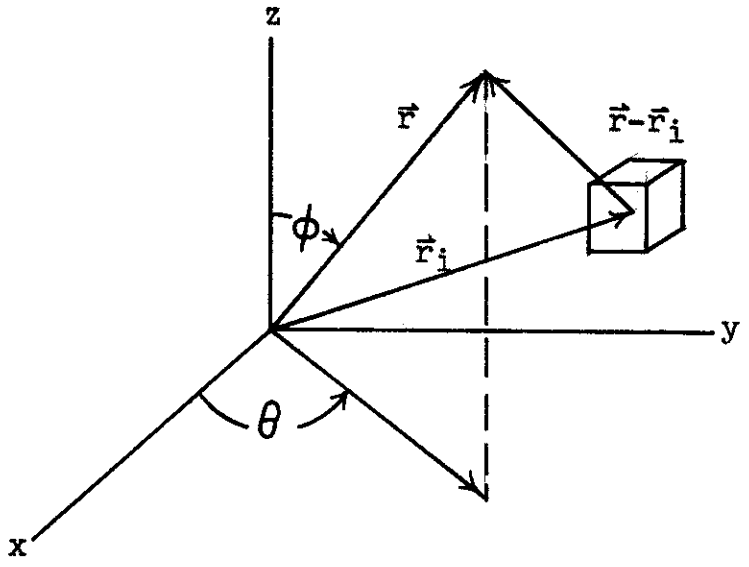

(a)

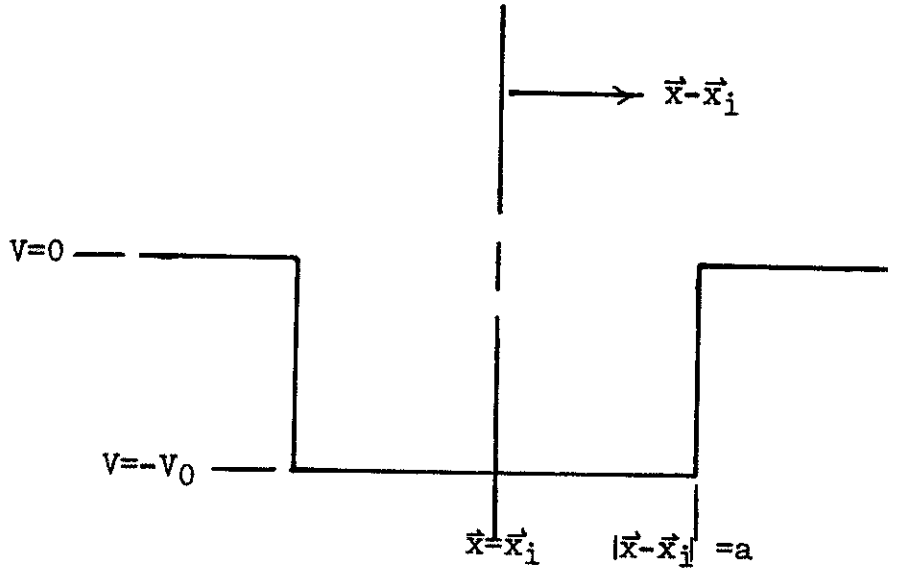

(b)

Fig. 3. Scattering center. (a) Coordinates of scattering center. (b) Scattering center potential for x direction.

After Eq. (26) is integrated, the matrix elements become

$$V_{\vec{K}\vec{K}'} = -4V_0|C|^2\sum_{i=1}^{N} \exp(iq_x x_i + iq_y y)\frac{\sin(q_x a)}{q_x}\frac{\sin(q_y a)}{q_y}$$

$$\times\left\{\frac{\sin[\pi(n-n')a/L]\cos[\pi(n-n')z_i/L]}{(n-n')(\pi/L)}\right.$$

$$\left.-\frac{\sin[\pi(n+n')a/L]\cos[\pi(n+n')z_i/L]}{(n+n')(\pi/L)}\right\}. \qquad (27)$$

The square of the potential matrix elements can be expressed as

$$|V_{\vec{K}\vec{K}'}|^2 = \gamma\sum_{i=1}^{N}\sum_{j=1}^{N}\exp[iq_x(x_i-x_j)+iq_y(y_i-y_j)]$$

$$\times\left\{\frac{\sin^2[\pi(n-n')a/L]}{[(n-n')(\pi/L)]^2}\cos[\pi(n-n')z_i/L]\cos[\pi(n-n')z_j/L]\right.$$

$$+\frac{\sin^2[\pi(n+n')a/L]}{[(n+n')(\pi/L)]^2}\cos[\pi(n+n')z_i/L]\cos[\pi(n+n')z_j/L]$$

$$-2\frac{\sin[\pi(n-n')a/L]\sin[\pi(n+n')a/L]}{(n-n')(n+n')(\pi/L)^2}\cos[\pi(n-n')z_i/L]$$

$$\left.\times\cos[\pi(n+n')z_j/L]\right\} \qquad (28)$$

where

$$\gamma = 16V_0^2|C|^4\frac{\sin^2(q_x a)}{q_x^2}\frac{\sin^2(q_y a)}{q_y^2}.$$

The average over the scattering coordinates is given by

$$\langle |V_{\vec{k}\vec{k}'}|^2 \rangle = \Omega^{-N} \int d\vec{r}_1 d\vec{r}_2 d\vec{r}_3 \cdots d\vec{r}_N |V_{\vec{k}\vec{k}'}|^2. \tag{29}$$

The terms in the integrand can be grouped according to their dependence on N. There are N terms where i = j, and $(N^2 - N)$ terms where $i \neq j$. Inserting Eq. (28) into Eq. (29) results in

$$\begin{aligned}
\langle |V_{\vec{k}\vec{k}'}|^2 \rangle = {} & \frac{N\gamma}{\Omega^N} \int d\vec{r}_1 d\vec{r}_2 d\vec{r}_3 \cdots d\vec{r}_N \left\{ \frac{\sin^2[\pi(n-n')a/L]\cos^2[\pi(n-n')Z_L/L]}{[\pi(n-n')/L]^2} \right. \\
& - 2\frac{\sin[\pi(n-n')a/L]\sin[\pi(n+n')a/L]\cos[\pi(n-n')Z_L/L]\cos[\pi(n+n')Z_L/L]}{[\pi(n-n')/L][\pi(n+n')/L]} \\
& \left. + \frac{\sin^2[\pi(n+n')a/L]\cos^2[\pi(n+n')Z_L/L]}{[\pi(n+n')/L]^2} \right\} \\
& + \frac{(N^2-N)\gamma}{\Omega^N} \int d\vec{r}_1 d\vec{r}_2 d\vec{r}_3 \cdots d\vec{r}_N \exp[iq_x(X_L - X_M) + iq_y(Y_L - Y_M)] \\
& \times \left\{ \frac{\sin^2[\pi(n-n')a/L]}{[\pi(n-n')/L]^2} \cos[\pi(n-n')Z_L/L]\cos[\pi(n-n')Z_M/L] \right. \\
& + \frac{\sin^2[\pi(n+n')a/L]}{[\pi(n+n')/L]^2} \cos[\pi(n+n')Z_L/L]\cos[\pi(n+n')Z_M/L] \\
& \left. - 2\frac{\sin[\pi(n-n')a/L]\sin[\pi(n+n')a/L]\cos[\pi(n-n')Z_L/L]\cos[\pi(n+n')Z_M/L]}{[\pi(n-n')/L][\pi(n+n')/L]} \right\}
\end{aligned} \tag{30}$$

where the subscripts L and M refer to any of the scattering coordinates. The $(N^2 - N)$ terms add to zero, thus reducing Eq. (30) to

$$\begin{aligned}
\langle |V_{\vec{k}\vec{k}'}|^2 \rangle = {} & 16N V_0^2 |C|^4 a^6 L (L-2a)^{-1} \\
& \times [(1 - q^2a^2/3)(1 + \delta_{nn'}/2) - \pi^2 a^2 (n^2 + n'^2)/(3L^2)]
\end{aligned} \tag{31}$$

with $q^2 = q_x^2 + q_y^2$.

The assumption is made that the defect size a is small compared to the sample thickness L and to the wavelength $1/k_\perp$. The trigonometric functions in Eq. (30) are expanded to keep terms to the order of a^4/L^4 and $a^4 k_\perp{}^4$. Equation (32) shows a typical expansion:

$$\frac{\sin(\alpha' a/L)}{\alpha' /L} \simeq a\left\{1 - \alpha'^2 (a/L)^2/6\right\}. \qquad (32)$$

For a bismuth sample these assumptions are justified, since the film thickness, in general, is greater than 200 Å, and the wavelength of an electron at the Fermi surface is about 600 Å. These numbers set the upper limit of a. For a metal the wavelength is about an angstrom, and the above assumption is marginal.[55]

CHAPTER V

VECTOR MEAN FREE PATH

Equation (14) gives $\vec{\Lambda}_{\vec{k}}$, the vector mean free path. This quantity must be calculated before the conductivity can be determined. Inserting Eq. (7) into Eq. (14) gives

$$\vec{\Lambda}_{\vec{k}} = \frac{\vec{v}_{\vec{k}}}{\langle v_{\vec{k}} \rangle} + \frac{2\pi}{\langle v_{\vec{k}} \rangle \hbar} \sum_{\vec{k}'} \langle |V_{\vec{k}\vec{k}'}|^2 \rangle \delta(E_{\vec{k}} - E_{\vec{k}'}) \vec{\Lambda}_{\vec{k}'} \tag{33}$$

where

$$\vec{\Lambda}_{\vec{k}'} \equiv \vec{\Lambda}(k_\perp', \theta', n'). \tag{34}$$

The symbol $\langle\ \rangle$ indicates the average over the scattering coordinates. Combining Eqs. (31) and (33) results in

$$\vec{\Lambda}_{\vec{k}} = \vec{v}_{\vec{k}} \langle v_{\vec{k}} \rangle^{-1} + 2\pi\beta \langle v_{\vec{k}} \rangle \hbar^{-1} \sum_{\vec{k}'} \left[(1 + \delta_{nn'}/2)(1 - q^2a^2/3) - \pi^2a^2/3L^2)^{-1}(n^2 + n'^2) \right] \times \vec{\Lambda}_{\vec{k}'} \delta(E_{\vec{k}} - E_{\vec{k}'}) \tag{35}$$

with

$$\beta = 16 N V_0^2 |c|^4 a^6/(L - 2a). \tag{36}$$

Then the vector mean free path becomes

$$\vec{\Lambda}(k_\perp, \theta, n) = \vec{v}_{\vec{k}} \langle v_{\vec{k}} \rangle^{-1} + \beta m^* A \langle v_{\vec{k}} \rangle^{-1} (2\pi\hbar^3)^{-1} \sum_{n'} \int_0^{2\pi} d\theta \int_0^{\infty} \left(\frac{\hbar^2}{2m^*} \right) dk_\perp'^2 \times \left\{ (1 + \delta_{nn'}/2) \left[1 - \frac{a^2}{3} \left(k_\perp^2 + k_\perp'^2 - 2k_\perp k_\perp' \cos(k_\perp, k_\perp') \right) \right] - \frac{\pi^2 a^2}{3L^2} (n^2 + n'^2) \right\} \times \vec{\Lambda}_{\vec{k}'} \delta(E_{\vec{k}} - E_{\vec{k}'}) \tag{37}$$

where the conversion

$$dK_\perp'^2 = 2K_\perp dK_\perp \tag{38}$$

has been used. Then Eq. (37) can be written

$$\vec{\Lambda}(K_\perp,\theta,n) = \vec{v}_{\vec{k}}\langle v_{\vec{k}}\rangle^{-1} + \langle v_{\vec{k}}\rangle^{-1}\frac{\beta m^* A}{2\pi\hbar^3}\sum_{n'}\int_0^{2\pi} d\theta\left\{1-\frac{a^2}{3}\left[2K_\perp^2+\frac{2m^*\alpha^2}{\hbar^2}(n^2+n'^2)\right]\right.$$

$$\left.+\frac{2a^2K_\perp}{3}\left(K_\perp^2+\frac{2m^*\alpha^2}{\hbar^2}(n^2-n'^2)\right)^{1/2}\cos(K_\perp,K_\perp')-\frac{\pi a^2}{3L^2}(n^2+n'^2)\right\}$$

$$\times\vec{\Lambda}\left(\left[K_\perp^2+\frac{2m^*\alpha^2}{\hbar^2}(n^2-n'^2)\right]^{1/2},\theta',n\right) + \langle v_{\vec{k}}\rangle^{-1}\frac{\beta m^* A}{4\pi\hbar^3}\int_0^{2\pi} d\theta'$$

$$\times\left\{1-2\frac{a^2}{3}K_\perp^2+2\frac{a^2}{3}K_\perp^2\cos(K_\perp,K_\perp')-\frac{2\pi^2a^2n^2}{3L^2}\right\}\vec{\Lambda}(K_\perp,\theta',n). \tag{39}$$

The function $\vec{F}_{\vec{K}_\perp,n}$ is defined by

$$\vec{F}_{\vec{K}_\perp,n} \equiv \int_0^{2\pi} d\theta\,\vec{\Lambda}(K_\perp,\theta,n). \tag{40}$$

Multiplying Eq. (39) by $d\theta$ and integrating over θ results in

$$\vec{F}_{\vec{K}_\perp,n} = \frac{\langle v_{\vec{k}}\rangle^{-1}\beta A}{2\hbar^3}\left(1-\frac{2a^2K_\perp^2}{3}-\frac{2\pi^2a^2n^2}{3L^2}\right)\vec{F} + \langle v_{\vec{k}}\rangle^{-1}\frac{\beta m^* A}{\hbar^3}$$

$$\times\left(1-2\frac{a^2K_\perp^2}{3}-\frac{2\pi^2a^2n^2}{3L^2}\right)\sum_{n'}\int d\theta'\,\Lambda\left(\left[K_\perp^2+\frac{2m^*\alpha^2}{\hbar^2}(n^2-n'^2)\right]^{1/2},\theta',n'\right)d\theta'. \tag{41}$$

The $\vec{v}_{\vec{k}}\langle v_{\vec{k}}\rangle^{-1}$ term in Eq. (39) can be expressed as

$$\int_0^{2\pi} d\theta\,\vec{v}_{\vec{k}}\langle v_{\vec{k}}\rangle^{-1} = \langle v_{\vec{k}}\rangle^{-1}\int_0^{2\pi} d\theta\,\frac{\hbar}{m^*}K_x. \tag{42}$$

The quantity $\langle U_{\vec{k}}\rangle^{-1}$ has no θ-dependence as can be seen from Eq. (A5) of the Appendix. Then Eq. (42) can be evaluated as

$$\langle U_{\vec{k}}\rangle^{-1}\int_0^{2\pi} d\theta \frac{\hbar}{m^*} K_x = \langle U_{\vec{k}}\rangle^{-1}\frac{\hbar}{m^*} K_\perp \int_0^{2\pi} d\theta \cos\theta = 0. \tag{43}$$

In a similar fashion the $\cos(k_\perp, k'_\perp)$ term integrates to zero. Equation (41) can be written

$$\sum_{n'}\int d\theta' \vec{\Lambda}\left(\left[k_\perp^2 + \frac{2m^*\alpha^2}{\hbar^2}(n^2-n'^2)\right]^{1/2}, \theta', n'\right) = \frac{\vec{F}_{\vec{K}_\perp, n}}{2}$$

$$\times\left[\frac{2\hbar^3}{\langle U_{\vec{k}}\rangle^{-1}\beta m^* A}\left(1 - \frac{2\alpha^2 k_\perp^2}{3} - \frac{2\pi^2\alpha^2 n^2}{3L^2}\right)^{-1} - 1\right]. \tag{44}$$

Thus Eq. (39) becomes

$$\vec{\Lambda}(K_\perp, \theta, n) = \vec{\Lambda}_{\vec{K}}\langle U_{\vec{k}}\rangle^{-1} + \langle U_{\vec{k}}\rangle^{-1}\frac{\beta m^* A}{2\pi\hbar^3}\sum_{n'}\left\{1 - \frac{\alpha^2}{3}\left[2k_\perp^2 + \frac{2m^*\alpha^2}{\hbar^2}(n^2-n'^2)\right]\right.$$

$$\left. - \frac{\pi^2\alpha^2}{3}(n^2+n'^2)\right\}\left[\frac{2\hbar^3}{\langle U_{\vec{k}}\rangle^{-1}\beta m^* A}\left(1 - \frac{2\alpha^2 k_\perp^2}{3} - \frac{2\pi^2\alpha^2 n^2}{3L^2}\right)^{-1} - 1\right]\frac{\vec{F}_{\vec{K}_\perp, n}}{2}$$

$$+ \langle U_{\vec{k}}\rangle^{-1}\frac{\beta m^* A}{3\pi\hbar^3}\sum_{n'}\frac{2\alpha^2 k_\perp^2}{3}\left[k_\perp^2 + \frac{2m^*\alpha^2}{\hbar^2}(n^2-n'^2)\right]^{-\frac{1}{2}}\int_0^{2\pi} d\theta' \cos(\vec{k}_\perp, \vec{k}'_\perp)$$

$$\times\vec{\Lambda}\left(\left[k_\perp^2 + \frac{2m^*\alpha^2}{\hbar^2}(n^2-n'^2)\right]^{1/2}, \theta', n'\right) + \langle U_{\vec{k}}\rangle^{-1}\frac{\beta m^* A}{4\pi\hbar^3}\left(1 - \frac{2\alpha^2 k_\perp^2}{3} - \frac{2\pi^2\alpha^2 n^2}{3L^2}\right)\vec{F}_{\vec{K}_\perp, n}$$

$$\langle U_{\vec{k}}\rangle^{-1}\frac{\beta m^* A}{4\pi^2\hbar^3}\frac{2\alpha^2 k_\perp^2}{3}\int_0^{2\pi} d\theta' \cos(\vec{K}_\perp, \vec{K}'_\perp)\vec{\Lambda}_\perp(K_\perp, \theta', n). \tag{45}$$

Inserting the first order approximation for $\vec{\Lambda}_{\vec{K}}$ from Eq. (33) into Eq. (40) results in

$$\vec{F}_{\vec{K}_\perp, n} = \frac{\hbar\vec{K}_\perp}{m^*\langle U_{\vec{k}}\rangle}\int_0^{2\pi}\cos\theta' d\theta' = 0. \tag{46}$$

Equation (39) then simplifies to

$$\vec{\Lambda}_{\vec{k}} = \vec{\nu}_{\vec{k}} \langle U_{\vec{k}} \rangle^{-1} + \langle U_{\vec{k}} \rangle^{-2} \frac{\beta m^* A}{2\pi\hbar^3} \sum_{n'} \frac{2a^2 k_\perp}{3} \left(k_\perp^2 + 2\frac{m^* a^2}{\hbar^2}(n^2 - n'^2) \right)$$
$$\times \frac{\hbar}{m^*} \int_0^{2\pi} d\theta' \cos\theta' \cos(k_\perp, k_{\perp'})$$
$$+ \langle U_{\vec{k}} \rangle^{-2} \frac{\beta m^* A}{2\pi\hbar^3} \frac{a^2 k_\perp^3 \hbar}{3 m^*} \int_0^{2\pi} d\theta' \cos\theta' \cos(k_\perp, k_{\perp'}). \tag{47}$$

Further evaluation results in

$$\vec{\Lambda}_{\vec{k}} = \vec{\nu}_{\vec{k}} \langle U_{\vec{k}} \rangle^{-1} + \langle U_{\vec{k}} \rangle^{-2} \frac{\beta A}{\hbar^2} \sum_{n'} \frac{a^2 k_\perp}{3} \left[k_\perp^2 + \frac{2m^* a^2}{\hbar^2}(n^2 - n'^2) \right] \cos\theta$$
$$+ \langle U_{\vec{k}} \rangle^{-2} \frac{\beta A a^2 k_\perp^3}{6\hbar^2} \cos\theta. \tag{48}$$

Even though the equation for $\vec{\Lambda}(k_\perp, \theta, n)$ was evaluated for some of the components of $\vec{k}$, the same result given in Eq. (48) can be achieved by simply making the first order approximation in Eq. (39). The scattering potential used in these calculations allows the additional terms to go to zero. For a δ-function potential such as used by Sandomirskii,[31] Eq. (48) reduces exactly to

$$\vec{\Lambda}_{\vec{k}} = \vec{\nu}_{\vec{k}} \langle U_{\vec{k}} \rangle^{-1} \tag{49}$$

after the first order approximation is made in Eq. (39).

CHAPTER VI

QUANTUM SIZE EFFECTS

The conductivity is calculated in Appendix B from Eq. (17). The results of the calculation are

$$\sigma = \frac{e^2\hbar^3(L-2a)n_e}{16\Omega m^{*2}(1+2[N_f])NV_0^2a^6|C|^4}\left\{1+\frac{5m^*a^2E_f}{3\hbar^2}-\frac{a^2\pi^2[N_f](1+[N_f])}{9L^2}\right.$$

$$-\frac{6\pi^2\hbar^2(1+[N_f])}{12m^*E_fL^2-\pi^2\hbar^2(2[N_f]+1)([N_f]+1)}$$

$$\left.\times\left[\frac{m^{*2}a^2E_f}{3\hbar^2}-\frac{\pi^2a^2(3[N_f]^2+3[N_f]-1)}{30L^2}\right]\right\}. \qquad (50)$$

The conductivity and the carrier concentration for an infinite sample are calculated in order to compare those quantities to those for a finite sample. From Appendixes C and D the conductivity for an infinite sample is

$$\sigma_\infty = \frac{e^2\hbar^3n_\infty}{64m^{*2}a^6n_{sc}V_0^2K_f\left(1-\frac{2a^2K_f^2}{3}\right)}\left[1+\frac{2a^2K_f^2}{9\left(1-\frac{2a^2K_f^2}{3}\right)}\right], \qquad (51)$$

and the electron concentration for an infinite sample is

$$n_\infty = (2E_fm^*)^{3/2}/(3\pi^2\hbar^3). \qquad (52)$$

The normalized carrier concentration n/n_∞ is given by combining Eqs. (23) and (52):

$$n/n_\infty = \frac{1}{4}\left(\frac{L_0}{L}\right)^3\left[\frac{L}{L_0}\right]\left\{6\left(\frac{L}{L_0}\right)-\left(\left[\frac{L}{L_0}\right]+1\right)\left(2\left[\frac{L}{L_0}\right]+1\right)\right\} \qquad (53)$$

where L_0 is a length equal to one-half the wavelength of a

particle at the Fermi surface. This characteristic length is determined by setting $[N_f]$ to its lowest nonzero value (1) and calling the film thickness L_0. Note that $n_e = 0$ if the film thickness is less than L_0. Under these conditions the discrete part of the energy alone is greater than the Fermi energy. Energies greater than the Fermi energy are excluded by the low temperature approximation. Equation (53) has been reduced to graphic form in Fig. 4. The oscillatory dependence of the carrier density on the sample thickness is clearly shown. The concentration is a continuous function of L; however, the derivation of n_e with respect to L does suffer discontinuities at $L = mL_0$ where $m = 1,2,3, \ldots$.

Equation (54) gives σ/σ_∞ as

$$\sigma/\sigma_\infty = \frac{2(L-2a)(n_e/n_\infty)K_f}{\pi(1+2[N_f])}\left\{1 - \frac{a^2K_f^2}{18} - \frac{a^2\pi^2[N_f](1+[N_f])}{9L^2}\right.$$

$$\left. - \frac{\pi^2a^2(1+[N_f])}{6L^2\left[\frac{2m^*E_fa^2}{\hbar^2} - \frac{\pi^2a^2}{6L^2}(1+[N_f])(1+2[N_f])\right]}\left[\frac{2m^*E_fa^2}{\hbar^2} - \frac{\pi^2a^2(3[N_f]^2+3[N_f]-1)}{5L^2}\right]\right\}. \quad (54)$$

The abrupt changes in the plot of σ/σ_∞ (see Fig. 5) are a demonstration of the QSE. There has been a general decrease in the conductivity, and the amplitude of the oscillations has decreased. A percentage decrease in the conductivity can be determined for each oscillation by comparing the conductivity maximum to the conductivity minimum. It is reasonable to assume that, though the amplitude of the oscillation has decreased as a result of an increase in

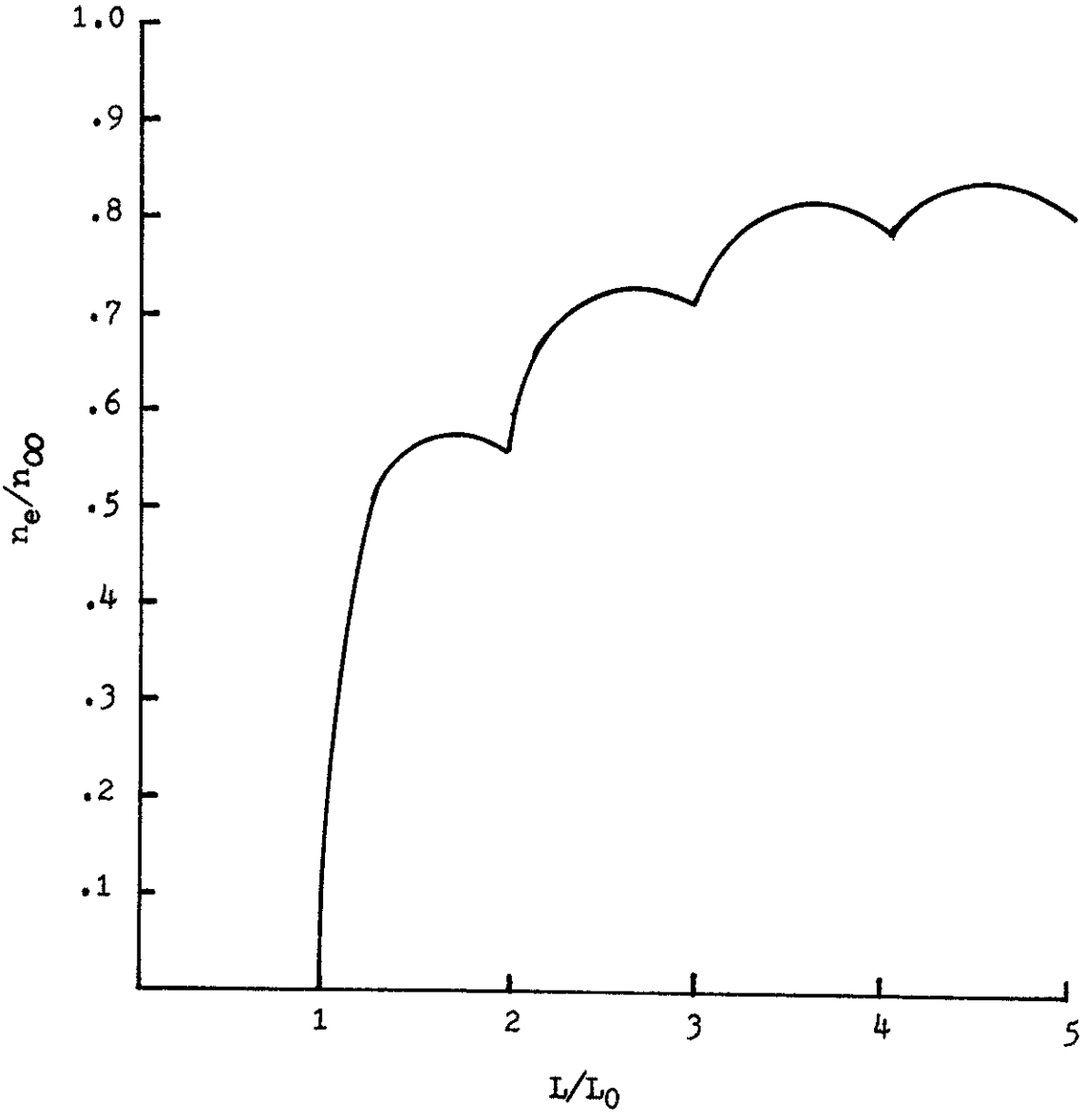

Fig. 4. Carrier density dependence on the sample thickness.

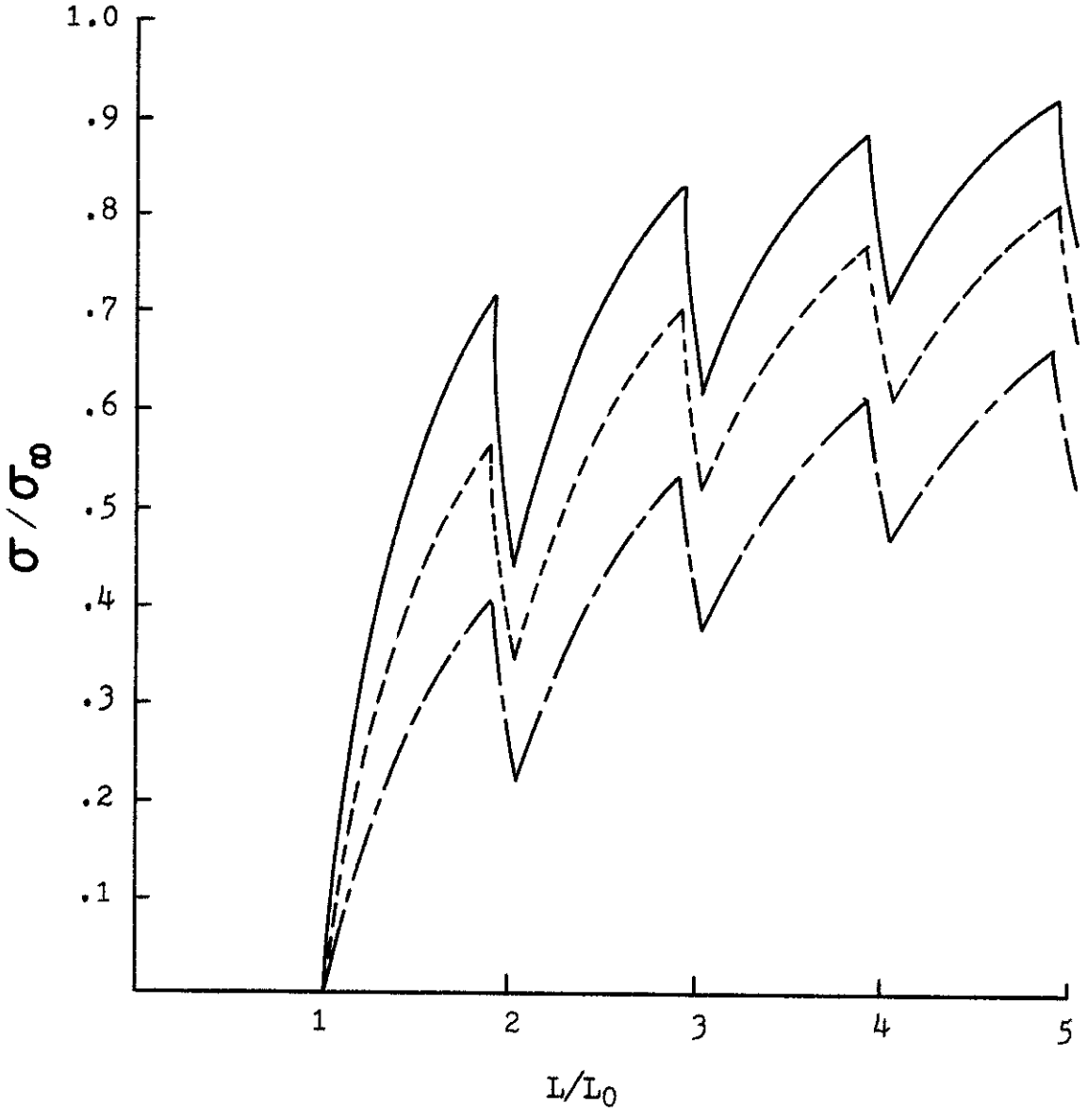

Fig. 5. Oscillatory dependence of electrical conductivity on thickness. ——, results when $\underline{a}$ is 0. ----, results when $\underline{a}$ is $L_0/(2\pi)$. — — —, results when $\underline{a}$ is L_0/π. The points at which the oscillations occur have been expanded so that the different curves may be seen.

scattering, the percentage of decrease will remain the same for each curve shown in Fig. 5. This is not the case, however, and an explanation is given in Chapter VII.

Sandomirskii's calculation[31] corresponds to the top curve in Fig. 5, i.e. a = 0. The sharp peaks in the oscillations are a result of the low temperature approximation. An expansion of the conductivity to finite temperature shows that the oscillation peaks round off very rapidly.[33] Sandomirskii's calculation was made using a δ-function potential and using the relaxation approximation in the Boltzmann equation. His results are included in Eq. (54) and can be recovered by allowing a to go to zero and $8a^3V_0$ to become constant. In this case the conductivity reduces to

$$\sigma/\sigma_\infty = \frac{2(L/L_0)\,n_e/n_\infty}{(1+2[\frac{L}{L_0}])}. \tag{55}$$

The conductivity curve for a = 0 in Fig. 5 shows the plot of Eq. (55).

A plot of Ogrin's experimental results for bismuth[7] is shown in Fig. 6. The period of the oscillations L_0 is 300-400 Å. Then the Fermi wavelength is $2L_0$. The effective mass is determined from the equation

$$m^* = \frac{k^2\pi^2}{2E_f L_0^2} \simeq .01\, m_0. \tag{56}$$

For bismuth the generally accepted value for E_f of .025 ev was used. Equation (56) gives an acceptable value for the effective mass.[5-7] The experimental results that have been

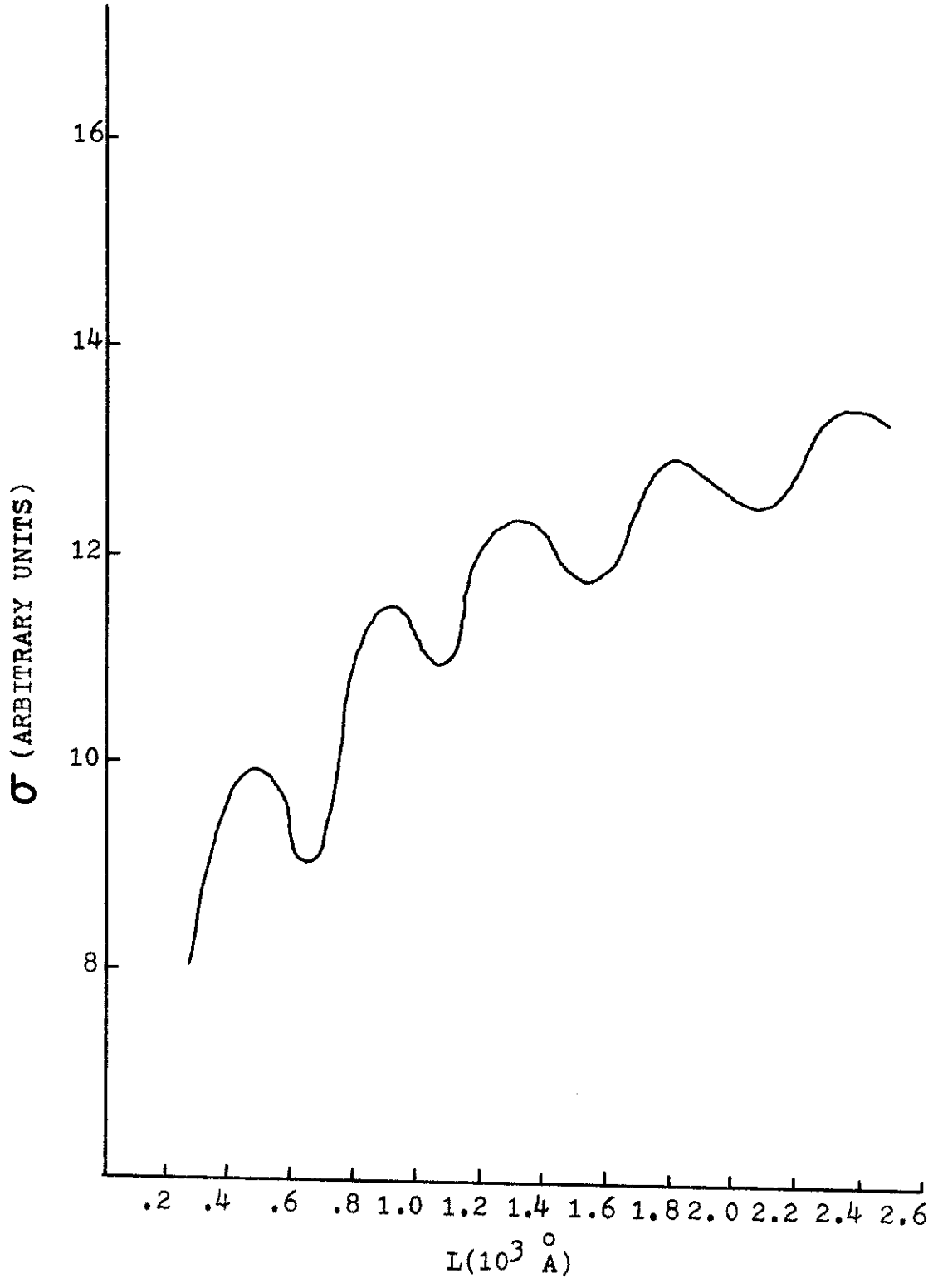

Fig. 6. Experimental QSE for bismuth. (Ogrin, Lutskii, and Elinson[7])

reported verify that the observed effects were those predicted by QSE theory.

The oscillatory effects in the carrier density and in the conductivity are a result of the constraints imposed on the density of electron states as a result of the finite sample. From Appendix E the density of states per unit volume is given as

$$\frac{\mathcal{D}(E)}{\Omega} = \frac{m^* [N_f]}{2\pi L \hbar^2} = m^* \left[\frac{L}{L_0}\right] (2\pi L \hbar^2)^{-1}. \qquad (57)$$

This equation is shown in graphic form in Fig. 7. The density of states for $L < L_0$ is zero as expected. At $L = L_0$ the density of states function is a maximum but decreases as L is further increased past L_0. The minimum in the state density curve increases as L increases, and eventually becomes independent of sample thickness. The state density, while providing useful information as well as insight into the problem, does not explain the decrease in the conductivity at each oscillation.

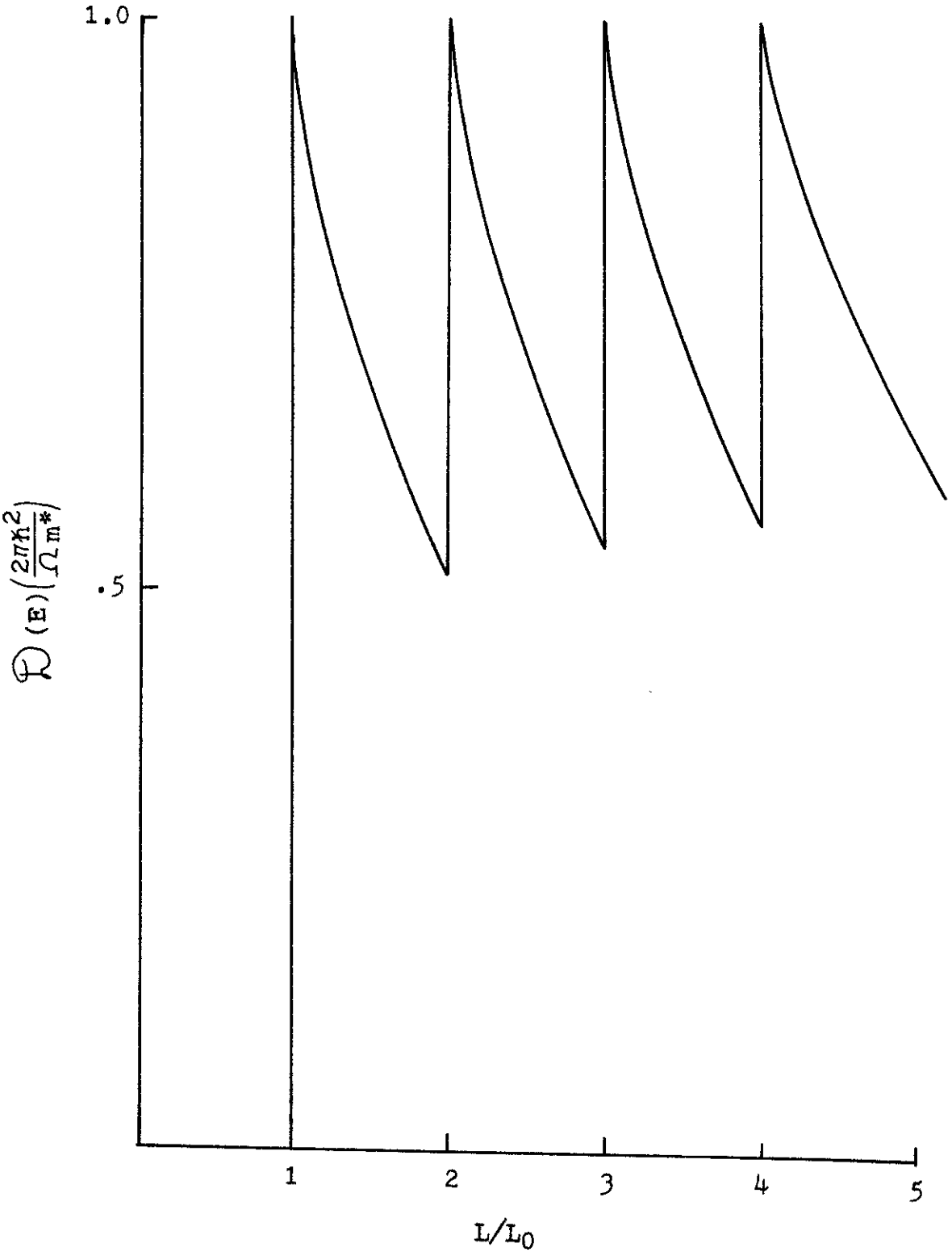

Fig. 7. Density of electron states per unit volume for a thin sample.

CHAPTER VII

DISCUSSION OF RESULTS

The overall decrease in conductivity due to increased scattering (see Fig. 5) reduces the absolute amplitude of the QSE oscillations. The percentage of change in the amplitude of the oscillations does not remain constant, as might be expected, but increases as the range of the interaction increases. The increase can be attributed to the scattering of electrons from conductive to nonconductive energy states.

The electron energy spectrum, Eq. (19), is composed of a discrete part and a continuous part. Figure 8 shows the variation of the discrete component of the energy with film thickness and shows the Fermi energy as constant. It is assumed that only electrons at the Fermi surface will contribute to the conductivity. The states for which the discrete part of the energy is approximately equal to the Fermi energy (i.e. $k_\perp \cong 0$) will contribute little to the current. Increasing L causes $k_\perp$ to increase. Both discrete and continuous energy levels will have some occupancy; hence the conductivity will be reduced but will remain finite each time a new energy band arrives at the Fermi surface. The low point in the conductivity oscillation is related to the transition probability from a state $(k_\perp, n)$ with a large $k_\perp$ component to

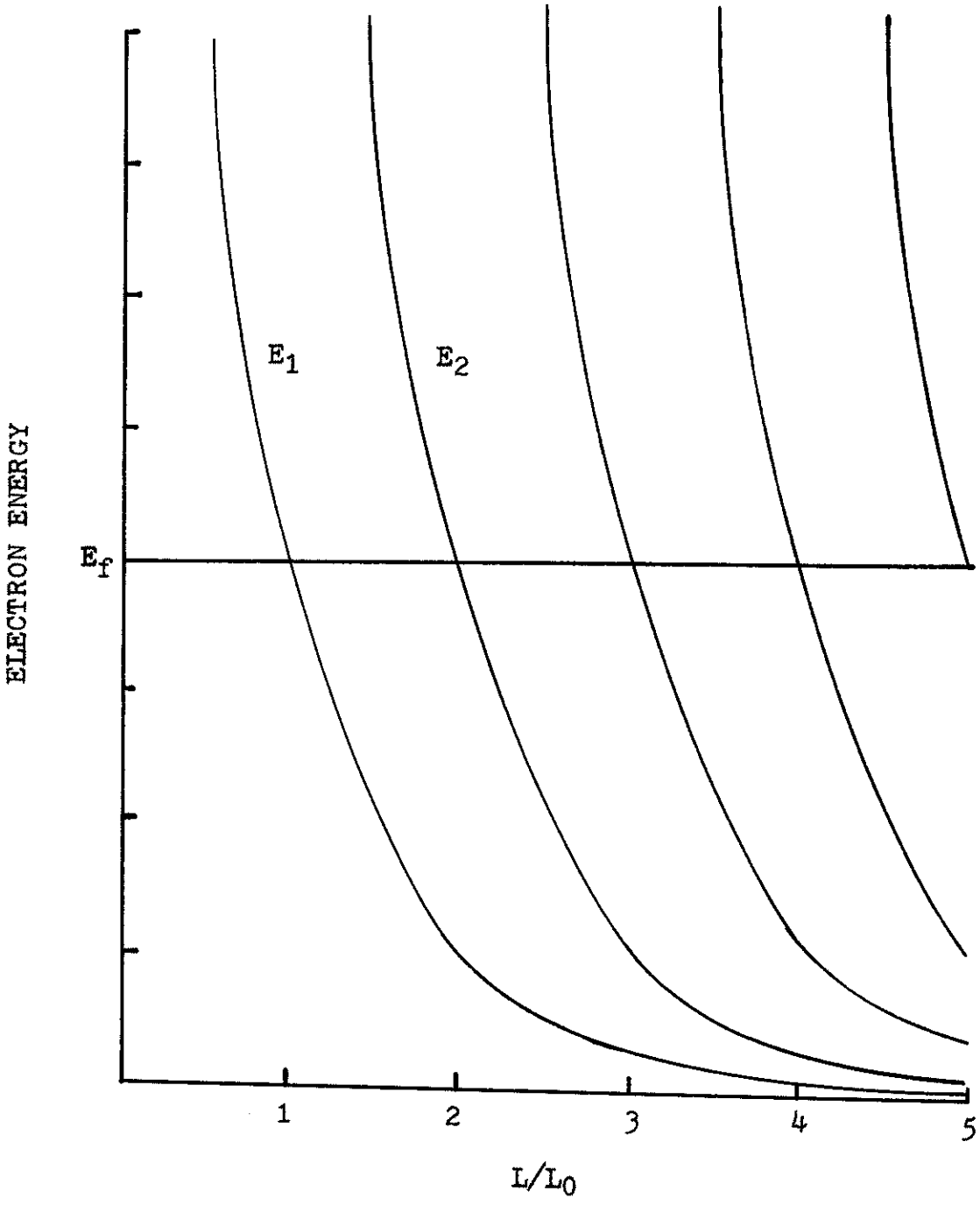

Fig. 8. The variation of the discrete part of the electron energy with thickness. The Fermi energy is denoted as E_f. Two different energy subbands are given by E_1 and E_2.

a state having a small $k_\perp$ component. As the film thickness is further increased, all available states have a nonzero $k_\perp$ component, and the conductivity increases accordingly.

Further insight into the influence of defects of finite volume on the amplitude of oscillations can be gained by computing the ratio R of the transition probability at $L = 2L_0$ from the conductive state $E_1(k_{\perp_1}, n = 1)$ to the conductive state $E_1(k_{\perp_2}, n = 1)$ to the transition probability from the conductive state $E_1(k_{\perp_1}, n = 1)$ to the nonconductive state $E_2(0, n = 2)$. Assuming the terms a/L and $ak_\perp$ to be small allows R to be calculated as shown in Eq. (58),

$$R = \frac{3}{2}\left[1 - \frac{\pi^2 a^2}{6L_0^2} + \frac{\pi^2 a^2}{2L_0^2}\cos(\theta_{1,2})\right] \tag{58}$$

where $\cos(\theta_{1,2})$ is the cosine of the angle between $k_{\perp_1}$ and $k_{\perp_2}$. An average over the scattering coordinate reduces the cosine term to zero.

The term R can be interpreted as the ratio of the number of electrons in a conductive state ($k_\perp \neq 0$) to the number of electrons in a nonconductive state ($k_\perp = 0$). Equation (58) can now be used to predict the change in the amplitude of the conductivity. A comparison of Eqs. (54) and (58) is shown in Table I for three values of $\underline{a}$ for $L = 2L_0$, and exceptional agreement is obtained.

TABLE I. Comparison of Eqs. (54) and (58) for the percentage of change in the amplitude of oscillations $\Delta\sigma/\sigma_\infty$ at a film thickness of $2L_0$ for three defect sizes.

Equation	a = 0	a = $L_0/(2\pi)$	a = L_0/π
(54)	40	41	46
(58)	40	41	44

CHAPTER VIII

CONCLUSIONS

In this theoretical investigation the effect of scattering from defects of finite size on the electrical conductivity of a thin semimetal slab is determined. Compared to δ-function scattering two changes in the conductivity occur. There is a general decrease in the conductivity, which is attributed to increased scattering. In addition, the amplitudes of the QSE oscillations are altered. This alteration is explained on the basis of scattering into available energy levels.

Several applications of the QSE have been suggested. A wedge-shaped semimetal film should exhibit a threshold characteristic in the current-voltage trace. A wedge-shaped semiconductor film, across which an electric field is applied, can be used as a light transformer.[42] Different conductivities in energy subbands that are associated with inversion layers in semiconductors can be utilized to form far infrared detectors.[56]

Further research should be directed toward understanding the temperature dependence of thin semimetals. The physical properties of a wide range of thin films should also be examined so that even more realistic results can be obtained.

APPENDIX A

CALCULATION OF $\langle U_{\bar{K}} \rangle$

From Eq. (14) the term $\langle U_{\bar{K}} \rangle$ is expressed as

$$\langle U_{\bar{K}} \rangle = \sum_{\bar{K}'} \langle Q(\bar{K},\bar{K}') \rangle$$

$$= \frac{2\pi}{\hbar} \sum_{\bar{K}'} \langle |V_{\bar{K}\bar{K}'}|^2 \rangle \, \delta(E_{\bar{K}} - E_{\bar{K}'}) . \qquad \text{(A1)}$$

Changing the summation to meet the requirements of this specific problem results in

$$\sum_{\bar{K}'} \longrightarrow \frac{A}{(2\pi)^2} \sum_{n'} \int d\bar{K}'_{\perp} = \frac{A}{(2\pi)^2} \sum_{n'} \int d\theta' \int K'_{\perp} \, dK'_{\perp}$$

$$= \frac{A}{2(2\pi)^2} \sum_{n'} \int d\theta' \int dK'^2_{\perp} . \qquad \text{(A2)}$$

Then Eq. (A1) becomes

$$\langle U_{\bar{K}} \rangle = \gamma' \sum_{n'} \int d\bar{K}'_{\perp} \left[(1 - q^2 a^2/3)(1 + \delta_{nn'}/2) \right.$$

$$\left. - \pi^2 a^2 (n^2 + n'^2)(3L^2)^{-1} \right] \delta(E_{\bar{K}} - E_{\bar{K}'}) \qquad \text{(A3)}$$

where

$$\gamma' = 8 A N V_0^2 |C|^4 a^6 L (L - 2a)^{-1} (\pi \hbar)^{-1}$$

and $\vec{q} = \vec{k}'_{\perp} - \vec{k}_{\perp}$. Further manipulation of Eq. (A3) gives

$$\langle U_{\vec{K}} \rangle = \frac{\gamma' m^*}{\hbar^2} \sum_{n'} \int_0^{2\pi} d\theta' \int_0^{\infty} \frac{\hbar^2}{2m^*} dk'_{\perp} \, \delta\left(\frac{\hbar^2}{2m^*} (K_{\perp}^2 - K_{\perp}'^2) + a^2 (n^2 - n'^2) \right)$$

$$\times \left\{ \left[1 + \delta_{nn'}/2 \right] \left[1 - \frac{a^2}{3} (K_{\perp}^2 + K_{\perp}'^2 - 2 K_{\perp} K_{\perp}' \cos(k_{\perp} k_{\perp}')) - \frac{\pi^2 a^2}{3L^2} (n^2 + n'^2) \right] \right\} \qquad \text{(A4)}$$

$$= \frac{8 m^* \Omega N V_0^2 |C|^4 a^6}{\hbar^3 (L - 2a)} \left[(1 + 2[N_k]) \left(\frac{1 - 2a^2 K_{\perp}^2}{3} \right) - \frac{4 a^2 \pi^2 n^2 [N_k]}{3L^2} \right] \qquad \text{(A5)}$$

where $[N_k]$ is the greatest integer function less than or equal to $(E_k/\alpha^2)^{\frac{1}{2}}$. This term arises from the δ-function

$$\delta\left(\frac{\hbar^2 k_\perp^2}{2m^*} + \alpha^2 n^2 - \frac{\hbar^2 k_\perp'^2}{2m^*} - \alpha^2 n'^2\right).$$

When $k'^2_\perp$ is evaluated, $(\hbar^2/2m^*)k_\perp^2 + \alpha^2 n^2 - \alpha^2 n'^2$ is set equal to $(\hbar^2/2m^*)k'^2_\perp$. For the maximum integer n'_M, $k'^2_\perp$ goes to zero. Then the maximum integer n'_M is less than or equal to $(E_k/\alpha^2)^{\frac{1}{2}}$.

APPENDIX B

EVALUATION OF THE CONDUCTIVITY

Combining Eqs. (17) and (48) results in

$$\vec{\sigma} = \frac{e^2}{\Omega}\sum_{\vec{K}} \vec{v}_{\vec{K}}\vec{v}_{\vec{K}}\langle U_{\vec{K}}\rangle^{-1}\delta(E_{\vec{f}}-E_{\vec{K}}) + \frac{e^2}{\Omega}\sum_{\substack{\vec{K}\\ \vec{K}'}} \vec{v}_{\vec{K}}\vec{v}_{\vec{K}'}\langle U_{\vec{K}}\rangle^{-1}\langle U_{\vec{K}'}\rangle^{-1}\langle Q(\vec{K},\vec{K}')\rangle\,\delta(E_{\vec{f}}-E_{\vec{K}}). \qquad \text{(B1)}$$

Inserting the results of Eq. (A5) into the first term of Eq. (B1) gives

$$\sigma_1 = \frac{e^2 A}{\Omega(2\pi)^2}\sum_n \int \frac{dk_\perp k_\perp^2 \cos^2\theta\;\delta(E_{\vec{f}}-E_{\vec{K}})}{\delta'\left[(1+2[N_K])\left(1-\frac{2a^2}{3}k_\perp^2\right)-\frac{4a^2\pi^2n^2[N_K]}{3L^2}\right]} \qquad \text{(B2)}$$

with

$$\delta' = \frac{8m^*\Omega N V_0^2 |C|^4 a^6}{\hbar^3(L-2a)}$$

and

$$\vec{v}_{\vec{K}} = \hbar\vec{K}_x/m^* = \hbar\vec{K}_\perp\cos\theta/m^*.$$

After integration, Eq. (B2) becomes

$$\sigma_1 = \frac{e^2\hbar^3(L-2a)n_e}{16\Omega m^{*2}(1+2[N_f])NV_0^2a^6|C|^4}\left\{1+\frac{2a^2}{3}\left(\frac{2m^*}{\hbar^2}\right)E_f - \frac{a^2\pi[N_f]}{6L^2n_e(1+2[N_f])}\right.$$
$$\left.\times\left[\frac{(1+[N_f])(1+2[N_f])}{6}\frac{2m^*E_f}{\hbar^2} - \frac{(1+[N_f])(1+2[N_f])(3[N_f]^2+3[N_f]-1)}{30L^2/\pi^2}\right]\right\}. \qquad \text{(B3)}$$

The second term in Eq. (B1) is

$$\sigma_2 = \frac{e^2}{\Omega}\sum_{\vec{K}} n_{\vec{K}}\langle U_{\vec{K}}\rangle^{-1}\delta(E_{\vec{f}}-E_{\vec{K}})\sum_{\vec{K}'}\frac{2\pi}{\hbar}\langle|V_{\vec{K}\vec{K}'}|^2\rangle\,\delta(E_{\vec{K}}-E_{\vec{K}'})\,n_{\vec{K}'}\langle U_{\vec{K}'}\rangle^{-1}. \qquad \text{(B4)}$$

The sum over $\vec{k}'$ in Eq. (B4) is evaluated as

$$\sum_{\vec{k}'} \langle |V_{\vec{k}\vec{k}'}|^2 \rangle \delta(E_{\vec{k}} - E_{\vec{k}'}) \nu_{\vec{k}'} \langle U_{\vec{k}'} \rangle^{-1}$$

$$= \frac{a^2 \hbar^2 k_\perp \cos\theta}{3\pi m^*} \sum_{n'} \int \frac{dk_\perp'^2 k_\perp'^2 (1 + \delta_{nn'}/2) \delta(E_{\vec{k}} - E_{\vec{k}'})}{(1+2[N])\left(1 - \frac{2a^2 k_\perp'^2}{3}\right) - \frac{2a^2 \pi^2 n'^2 2[N]}{3L^2(1+2[N])}} \tag{B5}$$

$$= \frac{2a^2 k_\perp \cos\theta}{3\pi}$$

$$\times \sum_{n'} \frac{(1 + \delta_{nn'}/2)\left(k_\perp^2 + \pi^2(n^2 - n'^2)/L^2\right)}{(1+2[N])\left[1 - \frac{2a^2}{3}\left(k_\perp^2 + \frac{\pi^2}{L^2}(n^2 - n'^2)\right) - \frac{4a^2\pi^2 n'^2 [N]}{3L^2(1+2[N])}\right]} \tag{B6}$$

$$= \frac{2a^2 k_\perp \cos\theta [N]}{3\pi(1+2[N])} \left\{ k_\perp^2 \left(1 + \frac{1}{2[N]}\right) + \frac{\pi^2}{L^2}\left(n^2 - \frac{(1+[N])(1+2[N])}{6}\right)\right\}. \tag{B7}$$

In Eq. (B7) the denominator is expanded for $a^2/L^2 < 1$. At this point σ_2 can be calculated. After integrating and summing the terms are grouped to give

$$\sigma_2 = \frac{e^2 \hbar^3 a^2 [N_f] (L - 2a) n}{24 m^{*2} \Omega (1+2[N_f]) N V_0^2 |C|^4 a^6} \left\{ \left[\frac{2m^* E_f}{\hbar^2} \right.\right.$$

$$- \frac{\pi^2 (1+[N_f])(1+2[N_f])}{6L^2} + \frac{m^* E_f}{[N_f]\hbar^2} \Bigg]$$

$$\left. - \frac{\pi (1+[N_f])(1+2[N_f])}{12 n L^2} \left[\frac{2m^* E_f}{\hbar^2} - \frac{\pi^2 (3[N_f]^2 + 3[N_f] - 1)}{5L^2} \right] \right\}. \tag{B8}$$

Inserting Eqs. (B3) and (B8) into Eq. (B2) and grouping gives the following results:

$$\sigma = \frac{e^2\hbar^3(L-2a)n_e}{16\Omega m^{*2}(1+2[N_f])NV_0^2a^6|C|^4}\left\{1+\frac{5m^*a^2E_f}{3\hbar^2}\right.$$

$$-\frac{a^2\pi^2[N_f](1+[N_f])}{9L^2}-\frac{3\pi^2\hbar^2(1+[N_f])}{6m^*E_fL^2-\pi^2\hbar^2(1+[N_f])(1+2[N_f])/2}$$

$$\left.\times\left[\frac{m^*a^2E_f}{3\hbar^2}-\frac{\pi^2a^2(3[N_f]^2+3[N_f]-1)}{30L^2}\right]\right\}. \qquad \text{(B9)}$$

APPENDIX C

CONDUCTIVITY FOR AN INFINITE SAMPLE

For an infinite sample the potential matrix elements are

$$V_{\bar{k}\bar{k}'} = -8V_0|C'|^2 \frac{\sin(q_x a)\sin(q_y a)\sin(q_z a)}{q_x q_y q_z} \sum_{i=1}^{N} e^{i\bar{q}\cdot\bar{r}_i} \qquad (C1)$$

where $q_x^2 + q_y^2 + q_z^2 = q^2$. Equation (C1) is averaged over the scattering coordinates to give

$$\langle |V_{\bar{k}\bar{k}'}|^2 \rangle = 64NV_0^2|C'|^4 \frac{\sin^2(q_x a)\sin^2(q_y a)\sin^2(q_z a)}{q_x^2 q_y^2 q_z^2}$$

$$= \gamma''(1 - q^2a^2/3) \qquad (C2)$$

where $\gamma'' = 64NV_0^2|C'|^4a^6$. Inserting Eq. (C2) into Eq. (14) results in

$$\langle U_{\bar{k}} \rangle = \frac{2\pi\gamma''}{\hbar} \sum_{\bar{k}'} (1 - q^2a^2/3)\delta(E_{\bar{k}} - E_{\bar{k}'})$$

$$= \frac{\gamma''\Omega}{\hbar(2\pi)^2} \int k'^2 \sin\phi' \left[1 - \frac{a^2}{3}(k^2 + k'^2 - 2kk'\cos(\bar{k}\bar{k}'))\right]$$

$$\times \delta(E_{\bar{k}} - E_{\bar{k}'}) d\theta' d\phi' dk'. \qquad (C3)$$

The relation between the angle $(\vec{k}\vec{k}')$ and other angles can be determined from Fig. 9:

$$K_x K'_x = KK'\sin\phi\cos\theta\sin\phi'\cos\theta'$$

$$K_y K'_y = KK'\sin\phi\sin\theta\sin\phi'\sin\theta'$$

$$K_z K'_z = KK'\cos\phi\cos\phi'. \qquad (C4)$$

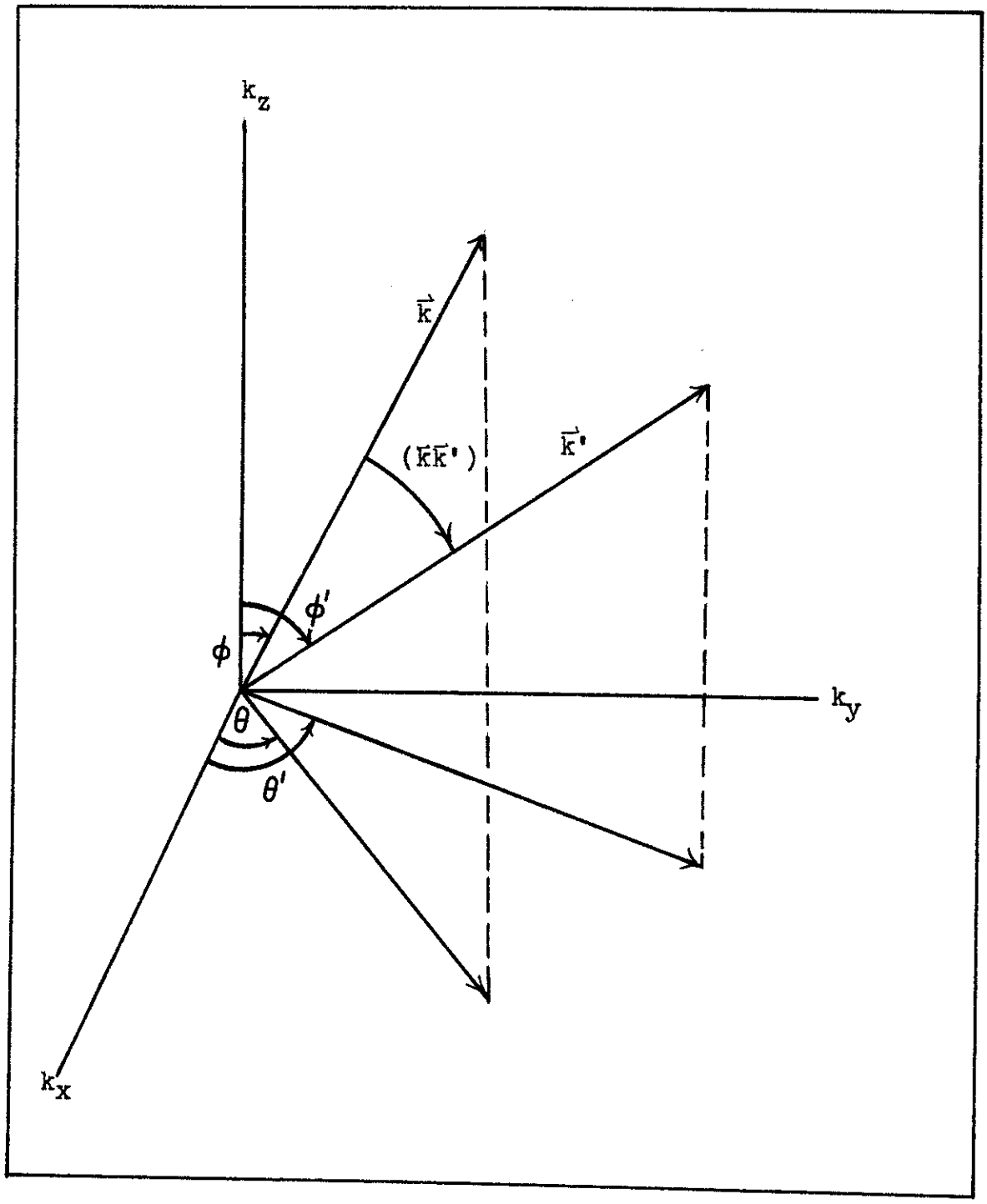

Fig. 9. Relation between $\vec{k}$ and $\vec{k}'$ in momentum space

The inner product between $\vec{k}$ and $\vec{k}'$ becomes

$$\vec{K}\cdot\vec{K'} = KK'\cos(\vec{K}\vec{K'}) = K_xK'_x + K_yK'_y + K_zK'_z. \tag{C5}$$

Combining Eqs. (C4) and (C5) results in

$$\cos(\vec{K}\vec{K'}) = \sin\phi'\sin\phi\cos(\theta-\theta') + \cos\phi\cos\phi'. \tag{C6}$$

Equation (C6) is used in the integration of Eq. (C3) to give the following:

$$\langle U_{\vec{k}}\rangle = \frac{\gamma'' \Omega K}{\hbar(2\pi)^2}\left(1 - \frac{2a^2K^2}{3}\right). \tag{C7}$$

The conductivity can be written as

$$\sigma = \sigma_1 + \sigma_2 \tag{C8}$$

with

$$\sigma_1 = \frac{e^2}{\Omega}\sum_{\vec{K}} \frac{v_{\vec{k}}^2}{\langle U_{\vec{k}}\rangle}\,\delta(E_{\vec{k}} - E_{\vec{f}}) \tag{C9}$$

$$= \frac{e^2\hbar^3K_f^2}{6\times 64\pi m^{*2}NV_0^2|C'|^4\Omega a^6(1-2a^2K_f^2/3)}. \tag{C10}$$

Equation (D3) gives the low temperature electron concentration as

$$n_\infty = \frac{K_f^3}{3\pi^2}. \tag{C11}$$

Then the first term in the conductivity is given by

$$\sigma_1 = \frac{e^2\hbar^3\pi n_\infty}{2\times 64\, m^{*2}NV_0^2|C'|^4\Omega a^6K_f(1-2a^2K_f^2/3)}. \tag{C12}$$

The second term in the conductivity is

$$\sigma_2 = \frac{e^2}{\Omega}\sum_{\substack{\bar{k}\\ \bar{k}'}} v_{\bar{k}} v_{\bar{k}'} \langle U_{\bar{k}}\rangle^{-1}\langle U_{\bar{k}'}\rangle^{-1} \langle Q(\bar{k},\bar{k}')\rangle\, \delta'(E_{\bar{f}} - E_{\bar{k}}) \tag{C13}$$

$$= \frac{e^2}{\Omega}\sum_{\bar{k}} v_{\bar{k}} \langle U_{\bar{k}}\rangle^{-1} \frac{\hbar}{2\pi m^*}\delta(E_{\bar{f}} - E_{\bar{k}})$$

$$\times \int \frac{d\bar{k}' \sin\phi' \cos\theta' (1 - q^2 a^2/3)}{(1 - 2a^2 k'^2/3)} \delta(E_{\bar{k}} - E_{\bar{k}'}) . \tag{C14}$$

Equation (C14) then becomes

$$\sigma_2 = \frac{e^2 \hbar^3 \pi k_f n_\infty a^2}{9 m^{*2} 64 N V_0^2 |C'|^4 a^6 \Omega (1 - 2a^2 k_f^2/3)^2} . \tag{C15}$$

Combining Eqs. (C8), (C10), and (C15) results in the following expression for the conductivity:

$$\sigma_\infty = \frac{e^2 \hbar^3 \pi n_\infty}{2 \times 64 m^{*2} N V_0^2 |C'|^4 a^6 \Omega (1 - 2a^2 k_f^2/3)} \left[\frac{1}{K} + \frac{2 k_f a^2}{9(1 - 2a^2 k_f^2/3)} \right] . \tag{C16}$$

APPENDIX D

ELECTRON CONCENTRATION FOR AN INFINITE SAMPLE

The total number of electrons in an infinite sample is given by

$$N_\infty = 2\sum_{\bar{k}} f(\bar{k}) \cong 2\sum_{\bar{k}} \Theta(E_{\bar{f}} - E_{\bar{k}}) \tag{D1}$$

$$= \frac{\Omega}{4\pi^3}\int_0^{k_f} dk\, d\theta\, d\phi\, k^2 \sin\phi\,. \tag{D2}$$

Then the electron concentration N_∞/Ω is given by

$$n_\infty = k_f^3/(3\pi^2)\,. \tag{D3}$$

APPENDIX E

ELECTRON STATE DENSITY

The number of electron states per unit energy range at low temperature is given by

$$\mathcal{D}(E) = \sum_{\bar{k}} \delta(E_{\bar{k}} - E_{\bar{f}}) \tag{E1}$$

$$= \frac{A}{(2\pi)^2} \sum_{n} \int d\bar{k}_\perp \, \delta(E_{\bar{k}} - E_{\bar{f}}) \tag{E2}$$

$$= \frac{A}{4\pi} \sum_{n} \frac{2m^*}{\hbar^2} \int \frac{\hbar^2}{2m^*} dk_\perp^2 \, \delta\left(E_{\bar{f}} - d^2n^2 - \frac{\hbar^2}{2m} k_\perp^2\right) \tag{E3}$$

$$= \frac{A m^*}{4\pi\hbar^2} \sum_{n=1}^{[N_f]} 1 \tag{E4}$$

$$= \frac{\Omega m^* [N_f]}{2\pi L \hbar^2} . \tag{E5}$$

REFERENCES

1. I. M. Lifshitz and M. I. Kaganov, Sov. Phys.--Usp. 2, 831 (1960).
2. I. M. Lifshitz and M. I. Kaganov, Sov. Phys.--Usp. 5, 878 (1963).
3. B. A. Tavger and V. Ya. Demikhovskii, Sov. Phys.--Solid State 5, 469 (1963).
4. V. B. Sandomirskii, Sov. Phys.--JETP 16, 1630 (1963).
5. Y. H. Kao, Phys. Rev. 129, 1122 (1963).
6. L. Esaki and P. J. Stiles, Phys. Rev. Lett. 14, 902 (1965).
7. Y. F. Ogrin, V. N. Lutskii, and M. I. Elinson, JETP Lett. 3, 71 (1966).
8. Yu. F. Komnik and E. I. Bukhshtab, JETP Lett. 6, 58 (1967).
9. N. E. Alekseevskii and S. I. Vedeneev, JETP Lett. 6, 302 (1967).
10. O. N. Filatov and I. A. Karpovich, JETP Lett. 10, 142 (1969).
11. F. Yu. Aliev, F. R. Godzhaev, I. G. Kerimov, and E. S. Krupnikov, JETP Lett. 13, 480 (1971).
12. F. F. Fang and W. E. Howard, Phys. Rev. Lett. 16, 797 (1966).

13. A. B. Fowler, F. F. Fang, W. E. Howard, and P. J. Stiles, Phys. Rev. Lett. 16, 901 (1966).

14. G. A. Antcliffe, R. T. Bate, and R. A. Reynolds, in The Physics of Semimetals and Narrow-Gap Semiconductors, edited by D. L. Carter and R. T. Bate (Pergamon Press, New York, 1971), p. 499.

15. E. Ugaz and H. H. Soonpaa, Solid State Commun. 6, 417 (1968).

16. V. P. Duggal, R. Rup, and P. Tripathi, Appl. Phys. Lett. 9, 293 (1966).

17. N. Garcia, Y. H. Kao, and M. Strongin, Phys. Rev. B 5, 2029 (1972).

18. Yu. A. Bogod and V. V. Eremenko, JETP Lett. 4, 114 (1966).

19. A. Lal and V. P. Duggal, Thin Solid Films 15, 157 (1973).

20. V. I. Vatamanyuk, Yu. A. Kulyupin, and O. G. Sarbei, JETP Lett. 7, 15 (1968).

21. V. N. Lutskii and L. A. Kulik, JETP Lett. 8, 80 (1968).

22. E. P. Fesenko, Sov. Phys.--Solid State 11, 2137 (1970).

23. E. P. Fesenko, Sov. Phys.--Solid State 11, 2135 (1970).

24. S. Konczak, S. Kochowski, and Z. Ziolowski, Thin Solid Films 17, 199 (1973).

25. Yu. F. Komnik and E. I. Bukhshtab, Sov. Phys.--JETP 27, 34 (1968).

26. H. Asahi, T. Humoto, and A. Kawazu, Phys. Rev. B 9, 3347 (1974).

27. Y. F. Ogrin, V. N. Lutskii, M. U. Arifova, V. I. Kovalev, V. B. Sandomirskii, and M. I. Elinson, Sov. Phys.--JETP 26, 714 (1968).

28. I. Gol'dfarb and B. A. Tavger, Sov. Phys.--Solid State 11, 1231 (1969).

29. P. N. Johnson and H. H. Soonpaa, in The Physics of Semimetals and Narrow-Gap Semiconductors, edited by D. L. Carter and R. T. Bate (Pergamon Press, New York, 1971), p. 121.

30. V. N. Lutskii, D. N. Korneev, and M. I. Elinson, JETP Lett. 4, 179 (1966).

31. V. B. Sandomirskii, Sov. Phys.--JETP 25, 101 (1967).

32. I. O. Kulik, JETP Lett. 5, 345 (1967).

33. S. S. Nedorezov, Sov. Phys.--JETP 32, 739 (1971).

34. M. Sh. Erukhimov and B. A. Tavger, Sov. Phys.--JETP 26, 560 (1968).

35. R. M. Krishnan and F. O. Meyer, III, Thin Solid Films (to be published).

36. A. Ya. Shik, Phys. Status Solidi 34, 661 (1969).

37. V. Bezak, J. Phys. Chem. Solids 27, 815 (1966).

38. V. Bezak, J. Phys. Chem. Solids 27, 821 (1966).

39. B. A. Tavger, Phys. Status Solidi 22, 31 (1967).

40. B. A. Tavger and V. Ya Demikhovskii, Sov. Phys.--Usp. 11, 644 (1969).

41. V. N. Lutskii, Phys. Status Solidi (a) 1, 199 (1970).

42. M. I. Elinson, V. A. Volkov, V. N. Lutskii, and T. N. Pinsker, Thin Solid Films 12, 383 (1972).

43. R. A. Hoffman and D. R. Frankl, Phys. Rev. B 3, 1825 (1971).

44. H. A. Combet and J. Y. Le Traon, Solid State Commun. 6, 85 (1968).

45. V. P. Duggal and R. Rup, J. Appl. Phys. 40, 492 (1969).

46. R. R. Schemmel and H. H. Soonpaa, Solid State Commun. 6, 757 (1968).

47. E. W. Fenton and J. P. Jan, in The Physics of Semimetals and Narrow-Gap Semiconductors, edited by D. L. Carter and R. T. Bate (Pergamon Press, New York, 1971), p. 115.

48. Yu. F. Komnik, E. I. Bukhshtab, Yu. V. Nikitin, and V. V. Andrievskii, Sov. Phys.--JETP 33, 364 (1971).

49. V. Ya. Demikhovskii and B. A. Tavger, Sov. Phys.--Solid State 6, 743 (1964).

50. N. S. Rytova, Sov. Phys.--Solid State 8, 1376 (1966).

51. J. Y. Le Traon and H. A. Combet, J. Phys. (Paris) 30, 419 (1969).

52. L. I. Schiff, Quantum Mechanics, 3rd ed. (McGraw-Hill Book Company, New York, 1968), Chap. 8, p. 244.

53. S. F. Edwards, Phil. Mag. 3, 1020 (1958).

54. P. L. Taylor, A Quantum Approach to the Solid State (Prentice-Hall, Inc., Englewood Cliffs, New Jersey, 1970), Chap. 8, p. 284.

55. C. Kittel, Introduction to Solid State Physics, 3rd ed. (John Wiley & Sons, Inc., New York, 1968), Chap. 7, p. 198.

56. R. T. Bate (private communication).